

We are IntechOpen, the world's leading publisher of Open Access books Built by scientists, for scientists

6,900

Open access books available

186,000

International authors and editors

200M

Downloads

Our authors are among the

154

Countries delivered to

TOP 1%

most cited scientists

12.2%

Contributors from top 500 universities



WEB OF SCIENCE™

Selection of our books indexed in the Book Citation Index
in Web of Science™ Core Collection (BKCI)

Interested in publishing with us?
Contact book.department@intechopen.com

Numbers displayed above are based on latest data collected.
For more information visit www.intechopen.com



Electrochemical Impedance Spectroscopy (EIS): A Review Study of Basic Aspects of the Corrosion Mechanism Applied to Steels

*Héctor Herrera Hernández, Adriana M. Ruiz Reynoso,
Juan C. Trinidad González, Carlos O. González Morán,
José G. Miranda Hernández, Araceli Mandujano Ruiz,
Jorge Morales Hernández and Ricardo Orozco Cruz*

Abstract

AC impedance measurements have been applied for over twenty years in electrochemistry and physics to investigate the electrical properties of conductive materials and their interfaces using an external electrical impulse (*VOLTAGE*, V or *CURRENT*, I) as driving force. Furthermore, its application has recently appeared to be destined in the Biotechnology field as an effective tool for rapid microbiologic diagnosis of living organism in situ. However, there is no doubt that the electrochemical impedance spectroscopy (EIS) is still one of the most useful techniques around the world for metal corrosion control and its monitoring. Corrosion has long been recognized as one of the most expensive stumbling blocks that concern many industries and government agencies, because it is a steel destructive phenomenon that occurs due to the chemical interaction with aqueous environments and takes place at the interface between metal and electrolyte producing an electrical charge transfer or ion diffusion process. Consequently, it is experimentally possible to determine through the EIS technique the mechanism and control that kinetics of corrosion reactions encounter. First, EIS data is collected through a potentiostat/galvanostat apparatus. After, it is fitted to a mathematical model (*i.e.* an equivalent electrical circuit, EEC) for its interpretation and analysis, fundamentally seeking a meaningful physical interpretation. Finally, this review reports some basic aspects of the corrosion mechanism applied to steels through the experimental EIS response using Nyquist or Bode plots. Examples are given for different applied electrochemical impedance cases in which steel is under study intentionally exposed to a corrosive aqueous solution by applying a sinusoidal potential at various test conditions.

Keywords: electrochemical impedance spectroscopy, corrosion process, charge transfer, electrical impulse, equivalent circuit, steels, chemical reactions

1. Introduction

Corrosion of steels represents worldwide, one of the most costly problems that several industries are challenged every day due to the aggressive conditions during the manufacturing process of the steel parts or the premature failure of steel tools by stress corrosion cracking (SCC) as well as deterioration of steel components from equipment and machinery in a certain service. The construction industry is an example in where steel is essential, which requires durable and strong structures for the build of bridges, tunnels, towers, buildings, airports, roads, plants and railways. Many of these constructions are usually outdoors, exposed to the atmosphere conditions, additionally, the surrounding environment where these steels are placed for their service is often highly polluted, that it often degrades the steel structure at a considerable corrosion rate. Some of those steels are also design to be used in the; mining industry, pipeline transport of fluids, shipbuilding, agriculture equipment and heavy machinery, among others. During their usage, steels are also severely damaged by one type of corrosion mechanism [1–4]. According to Zaki Ahmad [5] the concept of corrosion must be defined taking into account the environment in which the metal-materials are place to serve for long periods of exposure time, thus, all the environments are considered corrosive to some degree of damage as follows; i) air humidity, ii) fresh, distilled, salt and marine water, iii) natural urban, marine and industrial atmospheres, iv) steam and gases, v) ammonia and hydrogen sulfide, vi) sulfur dioxide and oxides of nitrogen, vii) fuel gases, acids, alkalis and soils.

Therefore, the concept of corrosion in steels is then define as a natural electrochemical process that destroys the integrity of the metal structure in the presence of any environment containing moisture and oxygen. This process involves two electrode reactions that can occur in a spontaneously way at the interface between the metal and the aqueous environment according to the thermodynamic's Law; One, is the reaction of metal-base with chemical species from the environment (*i.e.* anodic-oxidation reaction, which discharge electrons from the metal substrate) and the second is the reduction reaction of an oxidizing agent (*i.e.* cathodic reaction, which restores the electron deficiency with reduction of protons from the metal surface). The exchange of electrons between anodic and cathodic reactions produces an electronic current flow across the metal interface, which is known as corrosion potential (E_{corr}). This means the value at which the two-coupled reactions are in equilibrium, some effects can be caused by imposing an electrical potential on the metal surface as much greater than the E_{corr} to favored the metal dissolution reaction as a soluble species that diffuses into the aqueous solution [4, 5]. This suggests that Fe contained in steel as a base component is oxidized and depends on the free energy like a driving force of E_{corr} . The transfer of the charge (ions/electrons) through the metal interface, react with the oxygen from the steel surface, with the subsequent growth of an unstable corrosion product in the form of a thick porous-oxide layer (also known as rust), which occupies more volume than the original material. However, hydrated iron oxides are not considered as a protective layer on steels in presence of negative ions, Cl^- , SO_4^{2-} or NO_3^{2-} . **Figure 1** shows a typical example of the degradation mechanism of concrete structures due to corrosion of the steel reinforcement embedded in it; i) initially, the pores of the concrete structure are the access pathway of negative ions that come from the environment, ii) then, corrosion reduces the cross-sectional area of the steel bar, iii) it produces oxides (hydrated ferric oxide-rust) with a larger volume that cause tensile stress in surrounding concrete areas, which results in cracking and subsequent structural failure of the concrete [6].

In other conditions, a thin oxide film can grow on metal-base to provide the protection against corrosion attack, that steels require in order to be useful when

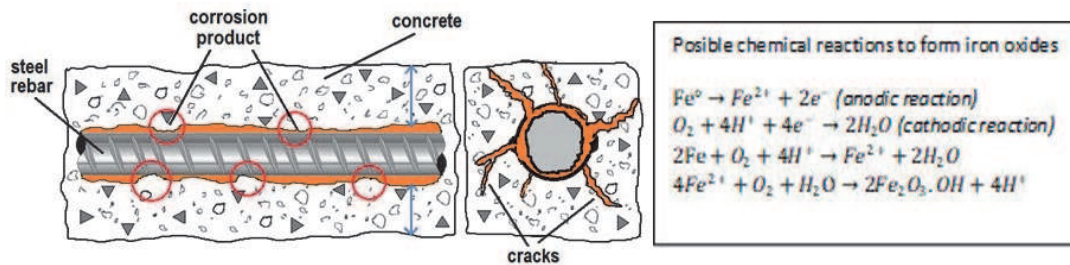


Figure 1.
 Physical and chemical model that represents the concrete failure by corrosion on the steel reinforcement [6].

they are exposed to severe atmospheric conditions during their usage. This passive film is so thin that it is invisible to the naked eye; however, this film can be self-repaired immediately, when it is suddenly scratched or intentionally removed. An example of this outstanding property is the existence of several types of stainless steels that usually contains a significant proportion of chromium (12 to 25 wt.% Cr) with nickel and molybdenum to prevent the formation of ferrous hydroxide ($\text{Fe}^{2+} + 2\text{OH}^- \rightarrow \text{Fe}(\text{OH})_2$ *rusting product*) by the presence of Cr in the Fe-base alloy, which reacts with oxygen from the environment to form a passive adherent oxide-layer (Cr_2O_3), thus, given a remarkably resistance to corrosion attack of the underlying metal, additionally, this oxide layer, can be regenerated by itself in the presence of oxygen [4, 7–9]. Based on the fundamental concepts, one of the advantages of using stainless steel is its high corrosion resistance, but in combination with other alloying elements can provide good mechanical strength, making the steel an appropriate material to be used in diverse applications that, in many cases, offers the only alternative for its high durability in aggressive environments; its use can be seen in domestic (cutlery, blades, household appliances and electronics), architectural (structures, handrails, concrete reinforcing bars, building components, cables for bridges and coastal works), transport (automotive exhaust system, ship containers, waste trucks and tankers for chemicals), chemical (pressure vessels, chemical containers, pipes, chemical plants, waste-water treatment), oil/gas (platform structures, machinery, storage tanks and pipelines), medical (surgical instruments, implants, equipment, dental inserts, wire and brackets in orthodontics), and other common uses (food containers, beverage bottles, springs, fasteners, bolts, nuts, washers and wires) [10].

For conventional steels produced by casting process, the most useful steel products are those that contain small amounts of alloying elements such as plain carbon steels (Mn, Si, S, P), alloyed steels (Cu, Ni, Cr or Al) and tool or machinery steels (W, Mo, Co, B and V). This alloying provides mechanical strength, ductility, machinability, and a substantial corrosion resistance. Although, these steels do not have the same ability of corrosion protection as the stainless steel does; the oxide film formed on the surface has only a few micrometers thick with microporous or growth defects, so it is possible to inferred that this oxide layer does not protect the metal from corrosion attack, this means a temporally low passivity is considered. However, in aggressive aqueous solutions the porous oxide layer can dissolve or break-down at least some areas of the film, therefore, leading to the Fe-base to a further localized attack. In industrial applications, the surface properties of the steel have a significant impact on their service life and performance. Among the several surface treatments to provide protection through a thick hard layer, diffusion techniques are using such as powder pack, gaseous atmosphere, plasma, ion beam and salt baths, that depends on the diffusion time and atmosphere concentration, these being a high effective treatment and less expensive. Additionally, carburizing, nitriding or boriding, are also well-known as thermochemical surface treatments [11–15].

Acid solutions are frequently used in many applications concerning industrial processes and are considered as the most corrosive media for steels. Acids like HCl, H₂SO₄, HNO₃, H₃PO₄, H₂CrO₃, and some alkalis such as NH₃ are frequently used for surface cleaning, removal of rust deposits, pickling processes, chemical attack, metal surface treatments, and wastewater systems. Other relevant uses are metal-processing equipment, chemical processing, pipelines, food processing, chemical and petrochemical plants. Therefore, printed research works report several cases of using organic molecules compounds (imidazole, 2mercapto-benzimidazole, pyridine, thidiazole, pyrrolidine, triazole, among others) that have provided a significant corrosion inhibition property for steels during their exposure to acid media [16–24]. These molecules must contain in their structure functional electronegative groups, π electrons, heteroatoms or heteroatoms of nitrogen, sulfur and oxygen with aromatic and heterocyclic rings. These reports generally indicate that the molecules are dissolved in an ethanol-water solution and then added in small concentrations (ppm) to the acid media, in all the cases, a barrier layer of organic molecules is formed onto the metal surface by an adsorption mechanism, thus giving corrosion protection on steels under-service at aggressive conditions [16, 18, 20, 24].

According to Florian B. Mansfeld (1988) in his research (*Do not be afraid of electrochemical techniques —But use them with care*) [25] comments that corrosion is fortunately a problem that can be tracked by means of electronic devices (*i.e.* potentiostats) that applies an electrical signal (V or I) to measure and control the electrical charge transfer; in pursuance of evaluating the reaction kinetic and mechanism of corrosion process that takes place at the metal interface. Meanwhile, the constant improvement of measuring instruments and the availability of commercial software, makes possible an easy performance of the electrochemical tests for the evaluation of corrosion progress and its control in an experimental way. These achievements caught the attention of chemical, petrochemical, food processing and steel manufacture industries, as well as research laboratories and higher education faculties that have encouraged and certified the success of the use of electrochemical techniques to monitoring corrosion on steels. The application of electrochemical techniques, such as linear polarization, polarization resistance and potentiodynamic polarization, have often been used for several decades in evaluating successfully some basic phenomena as oxide passivity, effects of alloying elements, reaction kinetics and the use of inhibitors to control the corrosion behavior, among others. However, it is important to consider the limitations of the polarization techniques that use Direct Current (DC), to perturb the equilibrium of the interface between the metal and electrolyte solution, is the ohmic-droop that is often ignored, this occurs when the current flows through the resistance of the test solution and the resistance of the connecting cables to electrochemical cell electrodes (*i.e.* uncompensated resistance, IR) [25]. The effects of IR can cause severe distortions of polarization curves, leading in the erroneous estimation of corrosion rates and misinformation of the kinetic model that represents the potentiodynamic curves. Given this limitation, through the last decade, another electrochemical technique appears to be more suitable for corrosion studies, this is the Electrochemical Impedance Spectroscopy (*EIS*) that uses a small amplitude of alternate current (AC) in a certain frequency domain applied to the corrosion system under study. Usually, *EIS* data is collected through a potentiostat/galvanostat apparatus, and then it is fitted to an equivalent electrical circuit (*EEC*) model for its interpretation and analysis, fundamentally seeking a meaningful physical interpretation. In correspondence with several studies [26–33] *EIS* is considered a successful new electrochemical technique with a great evolution in recent years that has become an

essential analytical tool in the research of materials science. For its detailed information, versatility and sensitivity that makes possible to be used widely in; corrosion studies and corrosion control, monitoring of properties of electronic and ionic conducting polymers or ceramics, colloids and coatings, measurements in semiconductors and solid electrolytes, studies of electrochemical kinetics at electrode-media interfaces, determination of conducting or diffusion mechanism, reactions and process [34].

The practical estimation of *EIS* technique could be difficult to understand by non-specialist because of the lack of comprehensive and explanation about the theory's basic aspects in conjunction with the experimental measurements. Nevertheless, it is possible to attain a logical interpretation and analysis of acquired impedance data for a certain practical system, such as those studied in this chapter that will be shown later. In this sense, to avoid uncertainties and misinterpretation of impedance data, analytical co-relationship of physical, chemical and manufacture parameters must be established with an equivalent electrical circuit (EEC) model, thus given a common sense to the impedance response. Therefore, this review considers a wide variety of practical electrochemical impedance cases for the study of corrosion mechanism on steels based on the basic aspects of *EIS* theory and its experimental interpretation. This chapter serves as a support for postgraduate students to have a criterion in deciding through their own experiences when using the electrochemical impedance technique. The practical cases discussed here are part of the research experienced by Dr. Héctor Herrera Hernández known in the scientific community as *DR.3H*. Recently, *DR.3H* and his students & research group are dedicated to their experience in electrochemical impedance knowledge in medical applications as bone replacement or PVDF-based membranes as an appropriate scaffold for skin cell growth [35].

Cases of *EIS* study applied to steels;

- Steels measured in their received condition.
- Kinetic oxidation reaction at different aqueous solutions.
- Steel corroded at non-stationary condition.
- Corrosion monitor in concrete reinforced materials.
- Inhibition using organic molecules.
- Inhibition in natural liquids extracted from plants.
- Hard-coatings as protection.
- Corrosion monitor in steels used as food containers or beverages.

1.1 Fundamentals of electrochemical impedance spectroscopy (EIS)

Since the middle of the 18th century, the Impedance Spectroscopy (IS) technique has been established as a popular theoretical approach to study the electrical properties of conducting materials and their interfaces. However, in the last quarter-century, IS becomes a practical tool that is successfully applied in electrochemistry as an analytical method widely used in many disciplines such as materials science, corrosion technology, semiconductors, conducting polymers,

ceramics, coatings, energy storage, and solid-state. Electrochemical Impedance Spectroscopy (EIS) is considered as a new technique with astounding advantages [36–38].

The concept of impedance in electronic devices is generally treated as a purely complex phenomenological amount and is considered as one of the most important physical characteristics that concerns the resistance that the medium opposes to the propagation of sound (acoustic impedance, Z) through it and therefore it is equivalent to the electrical impedance. In this sense, acoustic impedance is the ratio of the sound pressure of the wave (P) to its volume speed (U) in a material medium [39, 40]. This concept becomes a similar analogous meaning to the electric approach, because an electrical impulse (V or I) is applied to the conducting electrodes and a characteristic electrical response is resulted, known as impedance, Z . Therefore, impedance is then defined as the measure of the ability of a certain circuit to resist the flow of electrical current. The electrochemistry impedance is the relationship between a potential energy difference and the flow of electrons generated by a wave signal applied in an aqueous media. *EIS* technique is characterized by using an alternating current (AC) signal as driving force, which is applied to a conductive electrode, thus obtaining a characteristic response from the system interface. One of the attractive aspects that makes *EIS* as a suitable tool for investigating the electrochemical properties of materials during their exposure to aqueous solutions, is the simulation of the system behavior by means of an idealized circuit model. This consists of an arrangement of passive electrical components (*i.e.* resistors R , capacitors C and inductances L), which are the physical representation of the electrochemical processes occurring at the system interface under study.

Another quality of *EIS* is its high measurement sensitivity, which makes the technique an attractive advantage for detailed information that can be obtained from the system in study. For example, *EIS* was used to evaluate the properties of thin oxide films formed on metals, monitoring superficial degradation of polymer layers or paint coatings due to swelling process (coatings damaged by water uptake). Surface changes due to ion adsorption at the interface can also be detected, knowing the kinetics reaction on metals under corrosion process; all this, due to the advantages of this technique to perform measurements using a very small amplitude signal at variable frequency range. As result of the advantages mention above, *EIS* has attracted the interest of many scientist and engineers from different areas of application, for example: corrosion technology, electrochemistry, metallurgy, hydrodynamic, chemistry, biology, physics, mechanical, and medicine. According to organic chemistry a molecule is a group of non-electrically charged particles that have two or more atoms chemically bonded. They are components of the matter lying on earth (minerals, atmosphere, gaseous substances, organic and inorganic compounds, liquids, among others) [41]. Molecules can be measured with a small AC amplitude of voltage as a function of the frequency without altering their properties. Some systems leading to the formation of interfaces with the materials for example; a solid–solution interface allows the ion charge transfer, conduction and electron flow that is governed by the free energy of the chemical reactions occurring at the interface region (named double layer), as is shown in the model of **Figure 2**. The electrical properties of the double layer can be measured by an electrical equivalent circuit, considering that the double layer behave as pure capacitor C_{dl} (ions charge) and the flow of ions through the metal surface is view as a resistance R_{ct} of current, in according to Ohm's law. In general, *EIS* allows separating the contribution response of different components in terms of the resistance of electron charge transfer, double layer capacitance, solution resistance, inductance, and other parameters, where several electrochemical processes are proceeding at a different reaction rate.

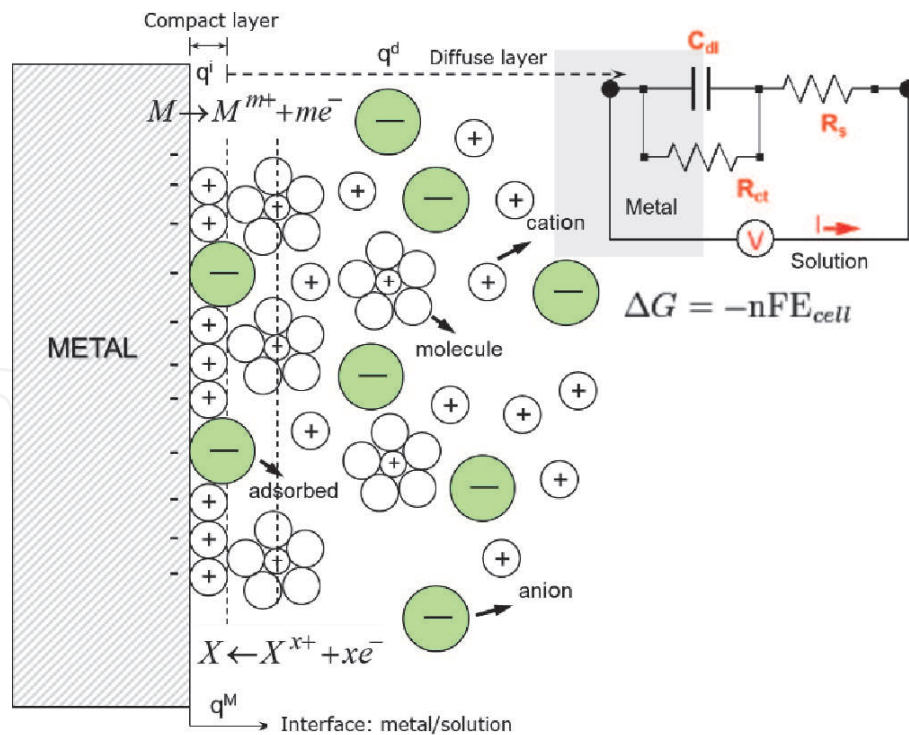


Figure 2. Schematic simulation of the electrochemical interface metal/electrolyte (electrical double layer) and its representative equivalent electrical circuit EEC model. R_s is the solution resistance, R_{ct} is the charge transfer resistance, C_{dl} is the capacity of the double layer.

1.2 Basics aspects of EIS data representation

Electrochemical impedance spectroscopy (EIS) is the analytical method widely used to study the electrochemical systems by applying a small AC voltage signal as a function of frequency of the amplitude signal. In potentiostatic mode as that of direct current (DC) techniques, like Linear Polarization Resistance (LPR) or Polarization Potentiodynamic, the basic measurement parameter is the polarization resistance R_p that is equal to the impedance (Z) in alternate current (AC) mode. This can be represented according to the Ohm's Law equation as denote bellow [8]:

$$R = \frac{V}{I} (DC), Z = \frac{E}{I} (AC) \quad (1)$$

where R is the resistor (Ω), V is the voltage (volts) and I is the current (amps) for direct current and E is the potential (volts) and Z is the impedance (Ω) for alternating current. To understand how the theory supports the EIS technique, it is necessary to consider two periodic waves; one is the current signal (I) and the other is related to potential signal (E). These waves behave as that shown in **Figure 3**, in which both signals oscillate at the same frequency and intensity, because one wave causes the other. However, there is an important effect that is the constant time shift between the two waves at certain angle, this is called the phase-angle shift (ϕ) and can vary from 0 to 90. Its unit is degrees ($^\circ$), because usually waves are considered vectors in a polar coordinate system or in a sine function. **Figure 3** shows the relation between waves E , I and the phase-angle shift. The applied sinusoidal perturbation can be a potential signal (E), thus given the measurement response in current (I) at a certain frequency domain. The excitation signal as a function of time t is represented as follows;

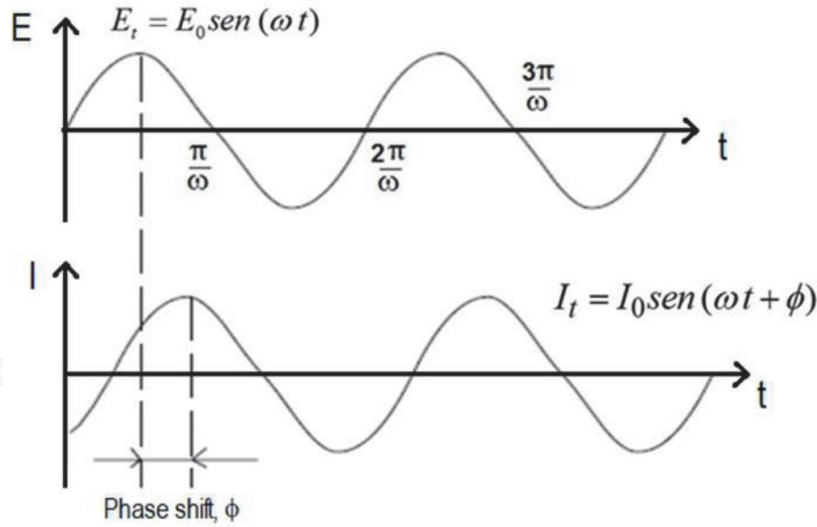


Figure 3.

Sinusoidal waveform response in linear system showing phase-shift angle that is used to describe the electrochemical reactions at the interfaces [42].

$$E_t = E_0 \sin(\omega t) \quad (2)$$

where E_t is the potential at time t , E_0 is the amplitude of the signal and ω is the angular frequency (expressed in terms of radians/second). So, the relationship between angular frequency and frequency (f in hertz units) is given by;

$$\omega = 2\pi f \quad (3)$$

in order to preserve the linear behavior in electrochemical systems, a small amplitude of AC voltage of about 5 to 10 mV is usually applied. I_t is the single response of instantaneous current at the maximum amplitude, Φ is the shifted-phase angle and has a different amplitude, I_0 as described in Eq. 4;

$$I_t = I_0 \sin(\omega t + \phi) \quad (4)$$

taking into account the electrical parameters of E and I as a function of angular frequency in the time domain, as well as the shifted-phase angle is possible to rearranged the Eq. 2 and 4 into Ohm's Law as DC current, this relationship enables to calculate the impedance of the system under study as follows;

$$Z = \frac{E(t)}{I(t)} = \frac{E_0 \sin(\omega t)}{I_0 \sin(\omega t + \phi)} = Z_0 \frac{\sin(\omega t)}{\sin(\omega t + \phi)} \quad (5)$$

then, impedance (Z_0) is defined as the ratio of applied voltage (E) divided by current (I) and represents an opposition to the flow of electrons or current in an AC circuit due to the presence of resistors, capacitors and inductors. Among of variety of passive electrical components, only resistors and capacitors or inductors contribute mainly to impedance; one is related to the real component (Z') and the other to the imaginary component (Z''). Due to this assumption, Z_0 can be expressed in its complex notation by incorporating the complex number $j = \sqrt{-1}$, where the **Figure 4** shows the complex representation of the impedance as vector concept, $Z(\omega) = Z' + jZ''$ and its phase-angle, $\tan(\phi) = \frac{Z''}{Z'}$. Using Euler relationship, the expression of the impedance translates in a complex function like;

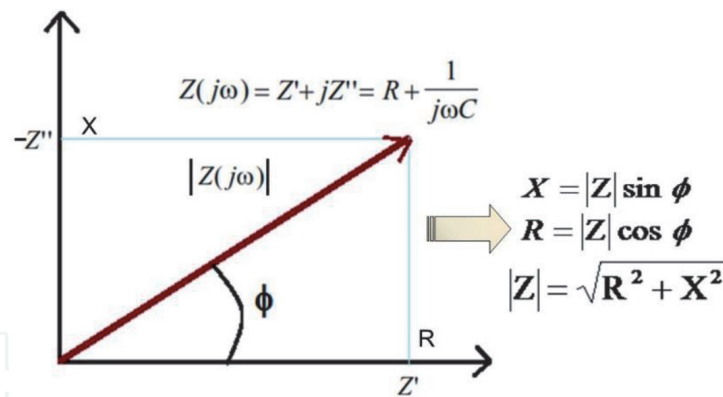


Figure 4. Vector representation of impedance as complex number; X capacitive-reactance, R resistance, Z' real component and Z'' imaginary part of impedance.

$$E_t = E_0 \exp(j\omega t), I_t = I_0 \exp(j\omega t - \phi) \quad (6)$$

considering the relationship between the potential and current amplitude, it results the total of the impedance as a complex number, as it follows;

$$Z(\omega) = \frac{E}{I} = Z_0 \exp(j\phi) = Z_0(\cos\phi + j\sin\phi) \quad (7)$$

however, the use of the current as a perturbation signal is also designed for certain electrochemical applications. Once the experimental data are collected, a series of potential-time and current-time are obtained, which correspond to the impedance at each frequency studied. The representation of the *EIS* data is by means of Impedance Spectra known as Nyquist Plots ($-Z_{\text{imag}}$ vs. Z_{real}) that represent the real impedance plotted against its imaginary part and also is often used the Bode plots ($\log|Z|$ vs. $\log \text{freq.}$, ϕ vs. $\log \text{freq.}$) that is the graphical representation of the modulus of the impedance and its phase-angle, as a function of the frequency domain) [43, 44]. However, Mansfeld [25] in his reports suggest that Bode plots is more appropriate to represent the impedance data because most of the measuring points are completely displayed at the entire frequency domain of the spectra. Thus, allowing a quick diagnosis of the behavior due to the sensitive of the phase-angle to small changes as a function of frequency variation, expecting time constants. While, Nyquist's diagrams are not recommendable since most of the data is grouped together at both ends of the spectra.

Experimentally speaking, when an *EIS* analysis is chosen to study the corrosion behavior of a piece of metal (*WE-working electrode*) that is immersed in an aqueous solution for a certain period of exposure time, which its equilibrium is perturbed by a low amplitude sinusoidal signal as function of frequency in the presence of a polarizable counter electrode (*CE*) and a reference electrode (*RE*), it is necessary to consider some electrical parameters (*i.e.* dielectric constant, permittivity, conductivity, resistivity and capacity charge) that will allow to interpret and deduce the corrosion behavior and its reactions mechanism by modeling the *EIS* data to an electrical *RC* circuit. These *RC* circuits are assembled with capacitors (*C*) and resistors (*R*) in parallel or series. C_{dl} is used to represent the electrical charge transfer at the metal/electrolyte interface known as the capacitance of a double layer (in farads), and that is present in all corroding aqueous systems. R_{ct} is the resistance of the electron charge transfer, which is the value of the impedance in its real component and R_s is the solution resistance. The combination of these three passive elements provides a simple equivalent electrical circuit (*EEC*) for a uniform

corroding metal. The experimental contribution of each parameter mentioned above is like that shown in **Figure 5**.

1.3 Analysis and interpretation of EIS spectra

As mention above, *EIS* data is usually represented by Bode plots in which the $|Z|$ module and phase angle ϕ are fuctions of frequency domain, sustained by its complex plane form that relates to Z_{real} with the imaginary part Z_{im} , and are usually interpreted by a mathematical correlation to a certain physico-electrical model known as equivalent electrical circuit (*EEC*), which is designed by an arrangement of ideal components (resistors R , capacitors C and inductors L) connected in series or parallel in order to reproduced the experimental *EIS* spectra. The impedance values of these elements are associated to the electrochemical processes of real systems such as electron charge transfer, diffusion processes, determination of the capacitance of the electrochemical double layer, mechanism of ions adsorption, mass transfer kinetic, characterization of coatings integrity, electrical resistance of the electrolyte, corrosion detection, conductivity, electrochemical reactions, among others, **Table 1** shows different *EEC* models that were designed to simulate & interpreted in particular some of the most common electrochemical processes, which will help to understand and describe the *EIS* spectra obtained during an experimental procedure. For example, If an alternating voltage $E(t) = E_o * \sin(\omega t)$ of about 10 mV at 1 Hz is applied to the *RC* circuits that are shown in **Table 1** as the perturbation energy of the models to carrier electrons through their passive components, this results in a signal that has a sinusoidal behavior and varies as a function on time (*i.e.* current intensity $I_o = \frac{E_o}{R}$), this waveform moves in the same direction and frequency as the supplied potential. However, to simplify the use of sinusoidal signals and their effect on different electrical components such as R (resistor), C (capacitor) and L (inductor), the typical sinusoidal response of the *RC* components is like that are shown in **Table 2**, and also it shows their relation to the shifted phase-angle value, the impedance as a function of time-frequency and their relationship to the electrochemical processes.

A single *RC* circuit is first considered to have only one ohmic resistance of 3.3 k Ω connected to a power source, in this case, the current intensity flows constantly through the resistor without any phase difference with respect to the potential that originates the waveform signal, $\phi = 0^\circ$. Then for this condition in that the phase-angle is equal to zero, the value of impedance module for a pure resistor (R) is relatively its reactive or real part ($Z_R(t) = R$), being its imaginary part or the

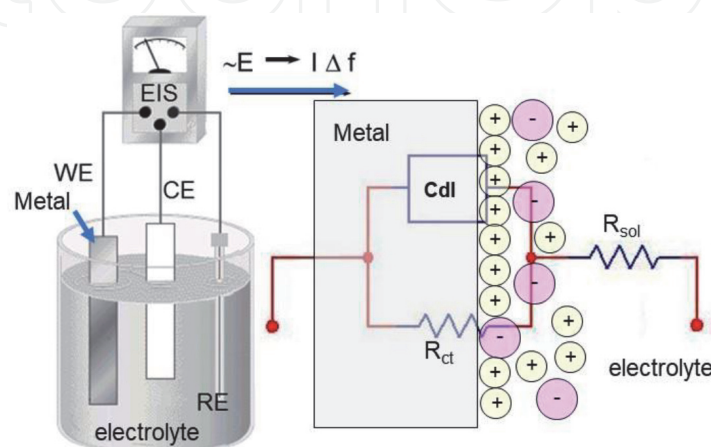


Figure 5.

Representation of a corrosion cell and its equivalent electrical circuit (*EEC*), WE is the working electrode, CE is the counter electrode and RE is the reference electrode.

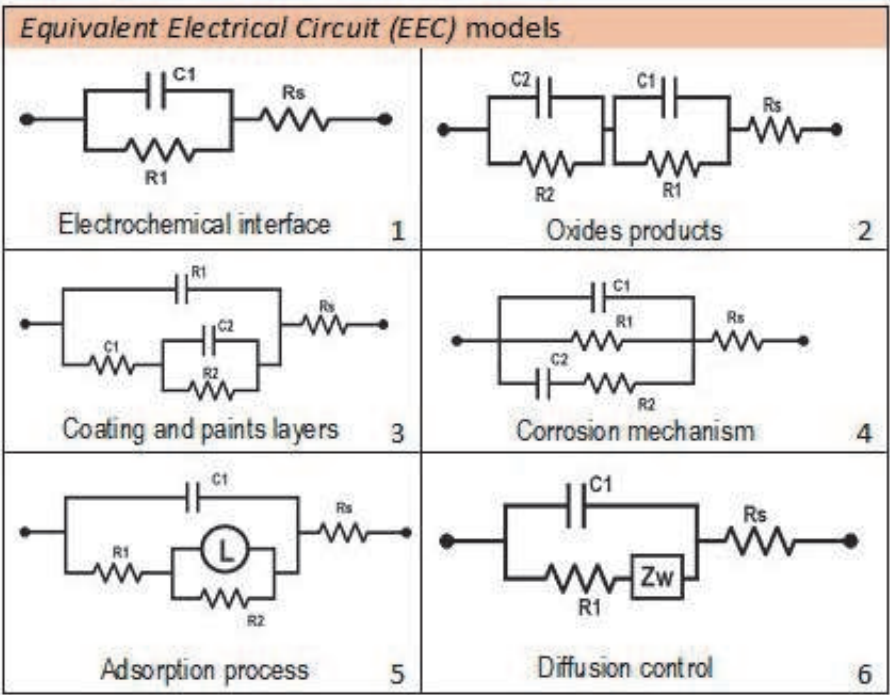


Table 1.
EEC models used to describe the electrochemical processes most studied by EIS. 1. Electrochemical interface (electron transfer), 2 and 3 oxide products and coatings, 4. corrosion mechanism, 5. adsorption and 6. ion diffusion processes.

Component	Description	Impedance, Z	Waveform signal
Resistor (R)	Is use to regulate the current flow trhough a particular path and obeys the Ohm's law (Ω).	$Z_R = R$ $\varphi_i = \varphi_v$	
Capacitor (C)	Component with capacity to store electrical charge q(t) in Faradios (F).	$Z_C = -\frac{1}{j\omega C}$ $\varphi_i = \varphi_v + 90^\circ$	
Inductor (L)	Coil of wire that induces a magnetic field as a result of current passing in henries (H).	$Z_L = j\omega L$ $\varphi_i = \varphi_v - 90^\circ$	

Table 2.
Impedance and phase shift angle response for the passive RC electrical components.

reactance X equal to zero, so it is suggested that this behaves as a resistive component. The impedance diagram for a resistive component shows a single straight line on its real axis that tends to infinity as dependent on time and frequency domain. In

the case of a pure capacitor (C) the sinusoidal response of voltage is retroceded at least by -90° allowing the imaginary component to be the variable dependent on time and frequency domain, so its value of $Z_C(t) = -\frac{1}{j\omega C}$. In the opposite case, it happens for an inductor (L) in which the current waveform signal is advanced near to 90° , which gives the expression $Z_L(t) = j\omega L$.

On the other hand, when two passive components are combined in a RC circuit, for example, one resistor of about 276Ω and a capacitor of $1 \mu F$ which are connected together in series, a small electrical AC signal of 10 mV is supplied to flow electrons through the closed circuit as dependence of frequency domain from 1 MHz to 1 mHz , the impedance is given by $Z_T(t) = -\frac{1}{j\omega C} + R_o$, and depending on the resistance and capacitor values can be considered as capacitive or resistive behavior. The Bode and Nyquist plots of **Figure 6a** show the experimental simulation of impedance response for these RC components connected both in series, which behave like a capacitive. Circuit model #1 shows the simplest arrangement of series and parallel, in which a resistor of $3.3 \text{ k}\Omega$ is connected in parallel to a capacitor of $1 \mu F$ and then in series with other resistance of 276Ω , its impedance response could be described as a function of frequency according to the following equation $\left(Z_T(t) = \frac{R_1}{1+(j\omega C_1 R_1)} + R_o\right)$, see **Figure 6b** the corresponding impedance spectra. So, circuit #1 is known as *Randles* circuit and is the typical electrical model used to described as analogy form the physical phenomenon of metal under corrosion attack [45, 46] by electron charge-transfer at the interface metal/electrolyte, and also to simulate uniform corrosion on homogeneous surface, which it has been the most used along the decades on researches. The information data of the impedance spectra is clearly visible in **Figure 6b**, because it is possible to obtain the value of the frequencies corresponding to the solution resistance R_s , charge transfer resistance R_{ct}

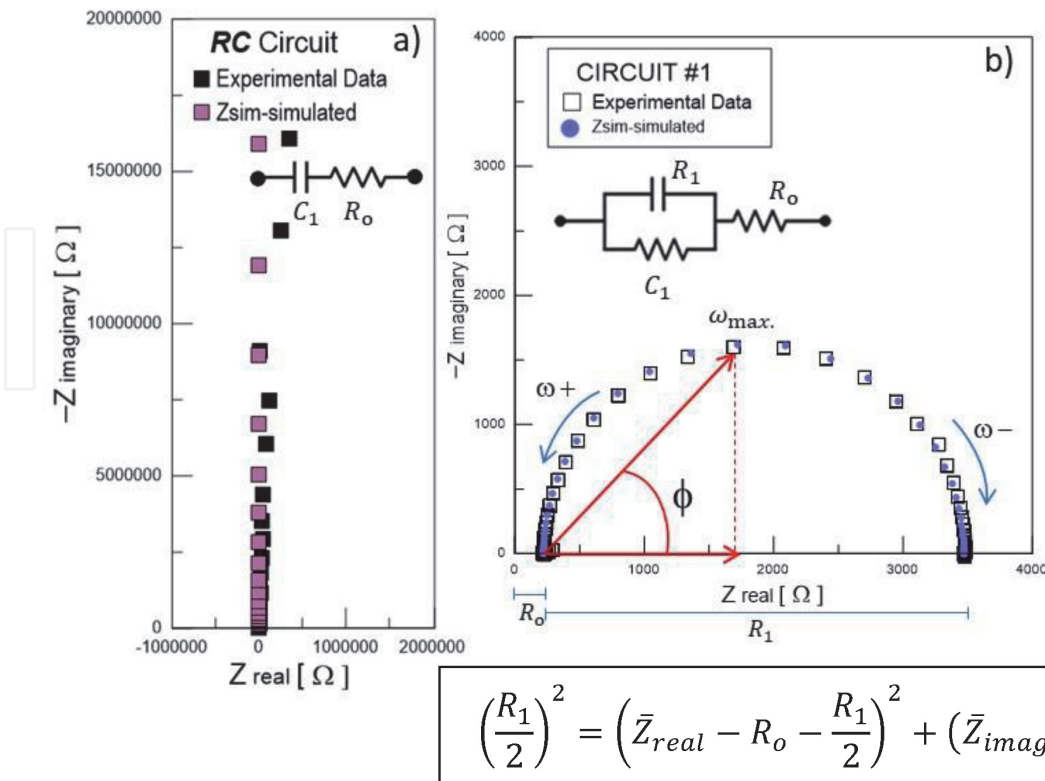


Figure 6. Impedance data simulation of a simplest EEC model; a) RC elements in series (high coating impedance) and b) circuit #1 RC in parallel follow by R in series (simple corrosion undergo by electron charge transfer). $R_o = 276 \Omega$, $R_1 = 3.3 \text{ k}\Omega$, $C_1 = 1 \mu F$.

(or polarization resistance), and its capacitance of the double layer C_{dl} . From the Nyquist Plot of **Figure 6b** C_{dl} is clearly observed as a well-defined semi-circle (*a single time constant*) in the entire frequency domain as results from the electrical circuit #1, which is the diameter of this semicircle is equal to R_{ct} and R_s is obtained by reading the real axis, Z' , value at the high frequency intercept. However, considering the maximum angular frequency (ω_{max}) as the frequency at which the imaginary component of the impedance Z'' has its largest value and R_{ct} , the value of C_{dl} is given by the following expression;

$$C_{dl} = \frac{1}{\omega_{max} R_{ct}} \quad (8)$$

Two-time constants could be expected in **Figure 7a** (circuit #2 is the combination of parallel RC in series) $\left(Z_T(t) = \frac{R_2}{1+j\omega C_2 R_2} + \frac{R_1}{1+j\omega C_1 R_1} + R_o\right)$, or **Figure 7b** (circuit #3 is a parallel arrangement in parallel connection $\left(Z_T(t) = \left\{ \left[\frac{R_2}{1+j\omega C_2} + R_1 \right] \parallel \frac{1}{j\omega C_1} \right\} + R_o\right)$ as results of applying voltage through the circuits or **Figure 7c** (circuit #4) $\left(Z_T(t) = \left[\left(R_2 + \frac{1}{j\omega C_2} \right) \parallel R_1 \parallel \frac{1}{j\omega C_1} \right] + R_o\right)$. These EEC models are used to describe the impedance spectra for oxide products forming by corrosion reactions on the metal surface, or anodizing coatings, or for paint-coated metals after exposed to corrosive electrolytes. Where C_1 is the capacitance of oxide film connected in parallel to R_1 that is the oxide resistance, both connected in series to RC parallel that contributes the electrical response of inner barrier layer or the double layer interface (oxide/metal matrix). The capacitance value of coating is measured in Farads [F], which depends on its dielectric constant ϵ and its thickness d as given by;

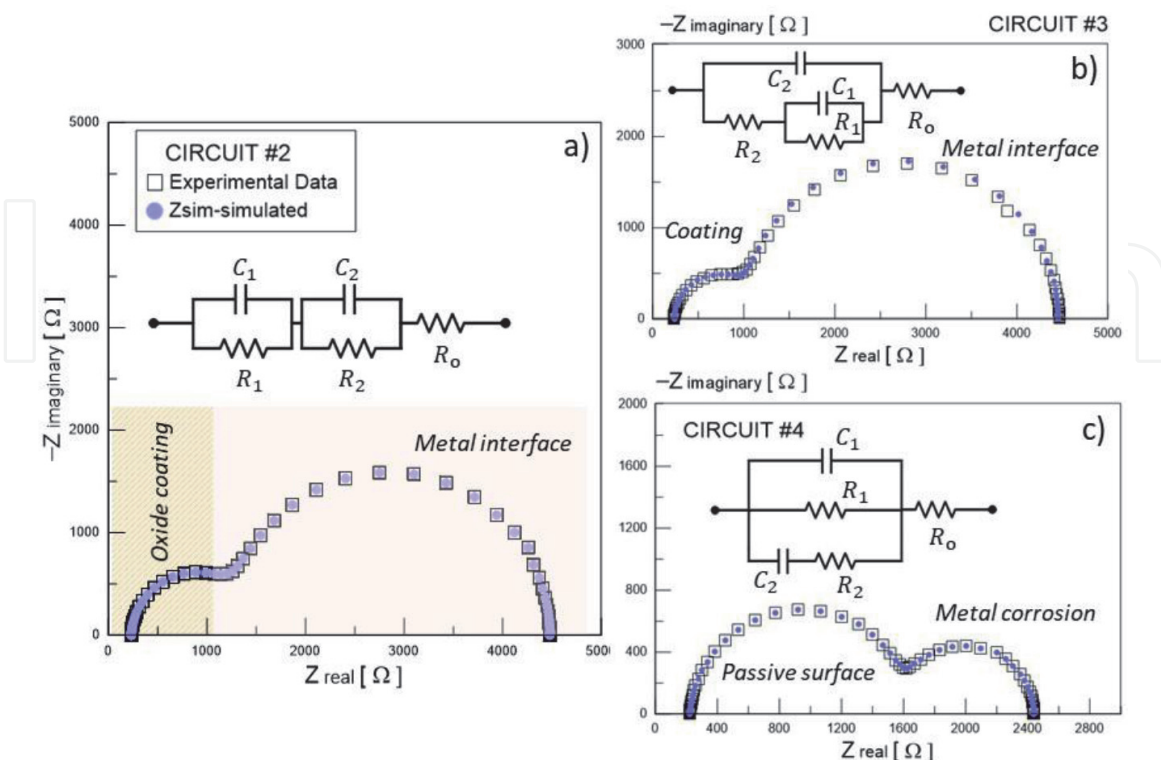


Figure 7. Impedance data simulation of EEC models; a) circuit #2 parallel RC elements in series (oxides products), b) circuit #3 parallel RC elements in parallel follow by R in series (paint coating) and c) circuit #4 parallel RC elements in series (corrosion mechanism). $R_o = 276 \, \Omega$, $R_1 = 3.3 \, k\Omega$, $C_1 = 1 \, \mu F$, $R_2 = 1 \, k\Omega$, $C_1 = 10 \, \mu F$.

$$C_c = \frac{\epsilon_o \epsilon A}{d} \quad (9)$$

Where ϵ_o is the electrical permittivity constant of free space (8.85×10^{-12} F/m) and A is the exposure area of the coated electrode. So, it is expected that the capacitance of coating increases with the exposure time due to water up-take by the coating through ionically conducting paths called pores. Changes in pores resistance and capacitance can be used to estimate the corroding metal.

Other types of impedance spectra commonly observed in the printed research works, are similar to that reproduced with the simulation using circuit #5 or #6. Circuit #5 is the similar arrangement of circuit #3, in which the ideal capacitor C is replaced by a magnetic coil (inductor) L ($Z_T(t) = \left[\left(\frac{j\omega R_2 L}{R_2 + j\omega L} + R_1 \right) \parallel \frac{1}{j\omega C_1} \right] + R_o$). In this sense the impedance diagram in **Figure 8** shows a semicircle very well defined by its diameter throughout the frequency range (charge transfer process) but is accompanied by a second inductance response below the semicircle at low frequencies, that means adsorption ion mechanism. This impedance response is commonly observed in electrochemical systems where chemical species, ion or any molecule is physically adsorbed at the interface of the electrochemical double layer with a given electrical charge motion. While circuit #7 is derived from the simplest circuit #1 in which its resistor is replaced by another electrical element

$Z_w \left(Z_T(t) = \frac{R_1 + W}{1 + [j\omega C_1 (R_1 + W)]^\alpha} + R_o \right)$ called Warburg impedance and related to the diffusion control of the species this can happen when the surface concentration of an electrochemically active species changes during the AC cycle. Thus, it must consider the impedance of a cathodic reaction, such as the reduction of oxygen that is common in corrosion systems. The general shape of a Warburg impedance is shown in **Figure 8b**. Two regions are clearly seen; a semicircle response is due to the charge transfer reaction and straight line with a 45° angle to the abscissa means to the diffusion of reactants [6, 43–45]. This is typical for analytical electrochemistry in diffusion controlled (W) in corrosion measurements, which is expressed by the Eq. (10), where σ is the Warburg coefficient and can be calculated from the slope of the straight line in the complex plane of **Figure 8b**.

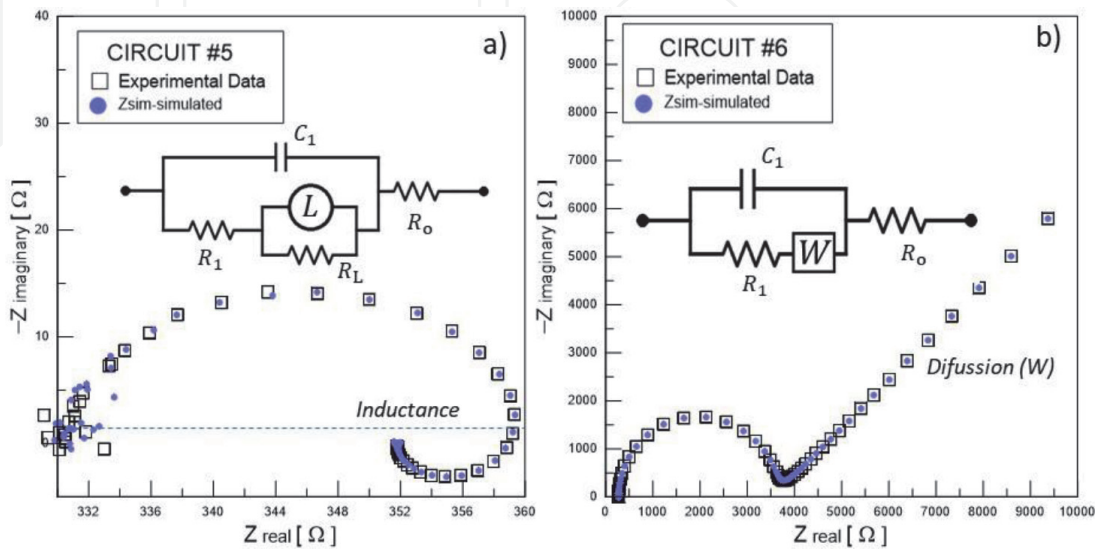


Figure 8. Impedance data simulation of EEC models; a) circuit #5 parallel RC elements in parallel with an inductance L (adsorption mechanism) and b) circuit #6 parallel RC elements in series with Warburg impedance W (diffusion control). $R_o = 276 \Omega$, $R_1 = 3.3 \text{ k}\Omega$, $C_1 = 1 \mu\text{F}$, $W_o = 0.001 \text{ S}\cdot\text{sec}^{0.5}$.

$$W = \sigma \omega^{-1/2(1-\alpha)} \tag{10}$$

In real cases the shape of Nyquist plot does not always show a perfect semicircle as it is observed for pure capacitor, it is necessary to replace capacitor (C) by a Constant Phase Element (CPE) in order to compensate the depression of the semicircle of frequency dispersion resulting of an experimental system due to the surface inhomogeneity, surface roughness, electrode porosity, surface disorder, geometric irregularities, and others. The CPE is a mathematical expression that is useful to represent several electric elements ($Z_{CPE} = \frac{Q_o}{(j\omega)^{1-\alpha}}$), [47]. To obtain the capacitance value (C_{dl}) from the CPE , it is necessary to obtain the maximum frequency of the Nyquist semicircle ($\omega_{\theta max}$) as well as the n exponent, this exponent can have values between 0.7 to 0.9, which can be used to describe the experimental data and a physical meaning is not yet clear, Q_o is a constant element with dimensions $S \cdot sec^n$. Eq. 11 shows the calculation of C_{dl} :

$$C_{dl} = Q_o * \omega_{\theta max}^{(n-1)} \tag{11}$$

In **Figure 9** is shown the configuration of EEC for a Nyquist Plot obtained experimentally from a corrosion system, the use of CPE was useful to adjust the experimental data to a mathematical fit in order to obtain the corrosion behavior of the metal (carbon steel APIX-52-5 L) in acidic media) $HCl1M$ [20, 47].
The validation of the parameters obtained through an analogous EEC model can be evaluated through the Kramers-Kronig Transformations (KKT), this is done in order to evaluate and understand the mechanisms that occur in the system interface. KKT are mathematical relationships between the real and the imaginary parts of the impedance that must be obeyed by valid impedance data. Therefore, meaning

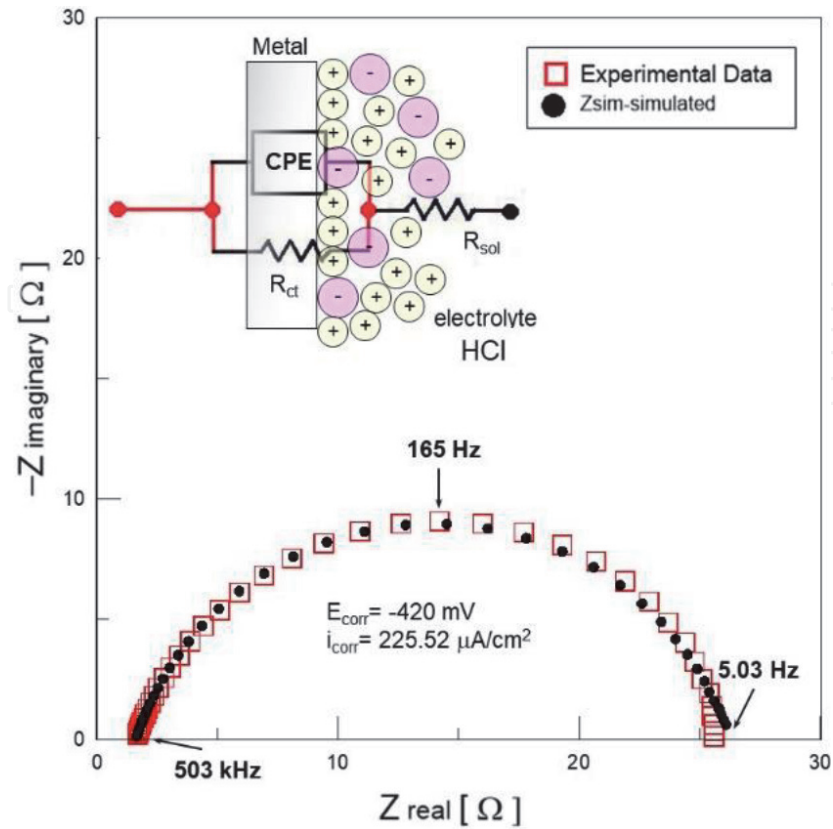


Figure 9.
 EEC electrical circuit #1 with a CPE to fit de impedance data corresponding to corrosion of pipeline steel immersed in HCl 1 M. $R_s = 1.58 \Omega \cdot cm^2$, $C_{dl} = 53.04 \mu F/cm^2$, $R_{ct} = 24.71 \Omega \cdot cm^2$.

that when imaginary impedance Z'' is known for all frequencies, it is possible to calculate the real impedance Z' at all frequencies [48, 49]. The general conditions on which *KKT* are based are show bellow:

1. Causality. The response of the system is due only to the perturbation applied and does not contain significant components from spurious sources.
2. Linearity. The perturbation and response of the system are linearly related *i.e.* the impedance is independent of the amplitude of the perturbation signal.
3. Stability. The system must be stable in the sense that it returns to its original state after the perturbation is removed.
4. The impedance must be finite-valued at $\omega \rightarrow 0$ and at $\omega \rightarrow \infty$ and must be continuous and finite-valued function at all intermediate frequencies.

It has been shown that when a corroding system obeys the just mentioned four criteria the impedance data will converse correctly. However, the inverse is not always true. It is still possible to have a correct *KKT* when impedance data are nonlinear. In the case of our impedance measurements we are mainly concerned about the stability of the system and for this case the *KKT* is an excellent tool for data validation.

2. EIS applied to metal corrosion

2.1 Analysis of effects of a voltage stimulus applied to corroded metals

One of the principal applications of *EIS* is in the study of electrolyte/electrode interfaces which is widely used in the evaluation of corrosion mechanism in metals at different environments conditions, but it has also been very useful in the performance of coatings [50–55] and in the failure detection of materials by stress corrosion cracking, similarly according to recent publications *EIS* also appears to be applied in ceramics materials [56–58]. In this sense, most of literature indicates that when applying a periodic signal of potential with amplitude from 5 to 10 mV in a given frequency domain, it is possible to detect the transitory current to obtain a change in the phase angle between I - V and the $|Z|$ data, which progress over time in order to predict metal corrosion phenomena or a possible electrochemical reactions at the metal interface. It should be noted that using a known electrical circuit it is possible to characterize the impedance spectra for each system under study as it shown before. The device that allows applying a programmed potential and detected the current is a potentiostat. Therefore, in this study a galvanostat-potentiostat PARSTAT-4000 was used to evaluate the effect of the voltage applied to the two-electrode interface. In which a periodic constant signal at 1 kHz of frequency was applied over a voltage range of 1 to 1000 mV as a function of frequency domain (1 MHz to 1 mHz). For this study it was considered the following systems; i) An ideal system like circuit #1, which is designed by RC components, a pure capacitor of 1 μF is connected in parallel to a resistor of 3 k Ω and then connected together in series with a resistor of 200 Ω and ii) a 3 cm² of stainless steel plate were used as working electrode (*WE*) after being exposed to an aqueous solution of HCl 1 M, then the *WE* was perturbed by a sinusoidal potential at different amplitude from 1 to 1000 mV, the corresponding impedance data for each of the cases that are displayed in **Figure 10**.

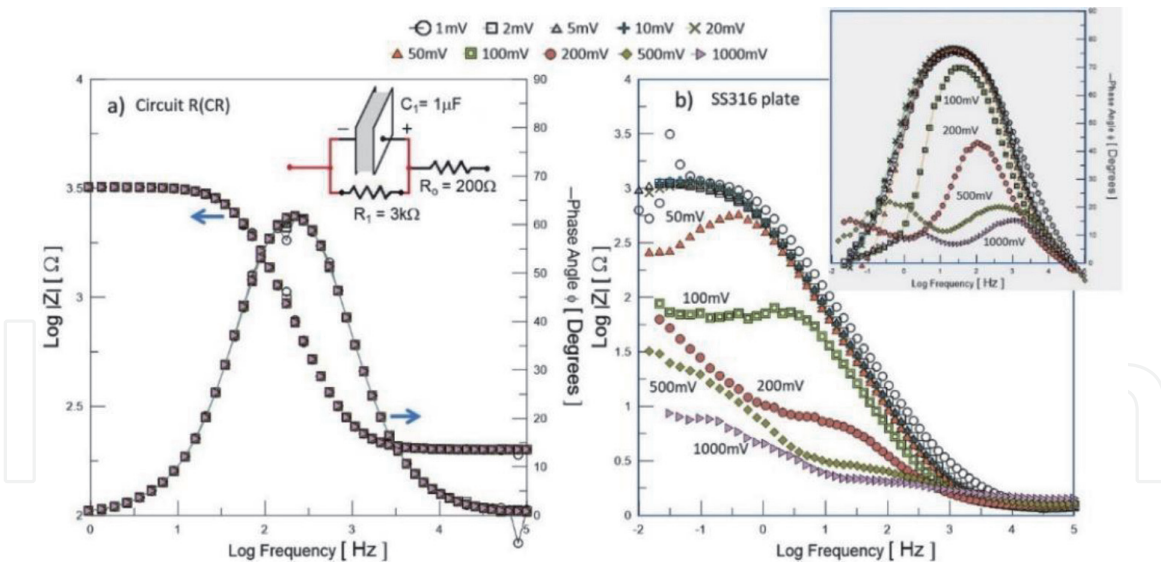


Figure 10.
 Typical impedance spectra showing the effects of the amplitude signal in; a) EEC model #1 ($R_0 = 276 \Omega$, $R_1 = 3.3 \text{ k}\Omega$, $C_1 = 1 \mu\text{F}$) and b) a stainless steel immersed in HCl 1 M.

The results show that when an alternate electrical pulse $V(t)$ of 1 kHz fluctuates from 1 to 1000 mV through an ideal circuit like EEC model #1 as that shown in **Figure 10a**, a uniform current $I(t)$ flows as a function of frequency domain, this signal produces a well-defined time constant in the entire frequency range. During the pulse at a time t the capacitor stores electrical energy causing an increase in potential difference ($Z_T(t) = \frac{q}{C}$) and that allows the current to be phase shifted with respect to the voltage of about 60° , meanwhile the resistor R_1 connected in parallel does not allow the passage of the current, instead of it decreases gradually to zero according to the Ohm's Law, that is why the capacitor stops charging load. Finally, when the period of the capacitor's transient load ends, the potential difference in the circuit must be zero when the stored load has been exhausted, *i.e.* the circuit has been returned to its equilibrium state. Due to the characteristics of the capacitor, which is composed by a parallel polished metal plates separated with a dielectric at a distance of d , and due to the transient events of charging rate and discharging rate during the continuous passage of the potential at different intensities of the signal amplitude does not cause changes in the interface of the plates, so the impedance data in bode representation are overlaid showing the same behavior for all data. That is, the load capacity or capacitance of $1 \mu\text{F}$ remains constant as the amplitude of the sinusoidal signal increases from 1 to 1000 mV as is shown in **Figure 11**.

The same behavior is observed for stainless steel SS316 plate immersed in HCl 1 M (**Figure 10b**), the metal interface exposed to the acid solution allows the electron transfer rate at the equilibrium potential (E_{corr}) after applying lower amplitudes of the stimulus signal (between 1 to 20 mV), the impedance diagrams for this conditions do not show changes caused by the current flows into the system. In this sense the metal interface working similar as the ideal capacitor allowing ions loading charging such as Cl^- and OH^- with capacitances ranging between 40 to $80 \mu\text{F}/\text{cm}^2$, which is indicated by a well-defined one time constant due to the presence of a protective oxide layer (passive condition) and can be easily represented by the EEC model #1. Notable effects can be caused by applying high current, as is clearly seen in the distortion of the shape of EIS diagrams during increasing the amplitude of the stimulus signal from 50 to 1000 mV, the impedance value $|Z|$ gradually down several orders of magnitude and severe changes in phase angle less than 20° are observed, this mean that two time constants are obvious seen and are related to the corroded interface, *i.e.* dissolution of the chrome protective

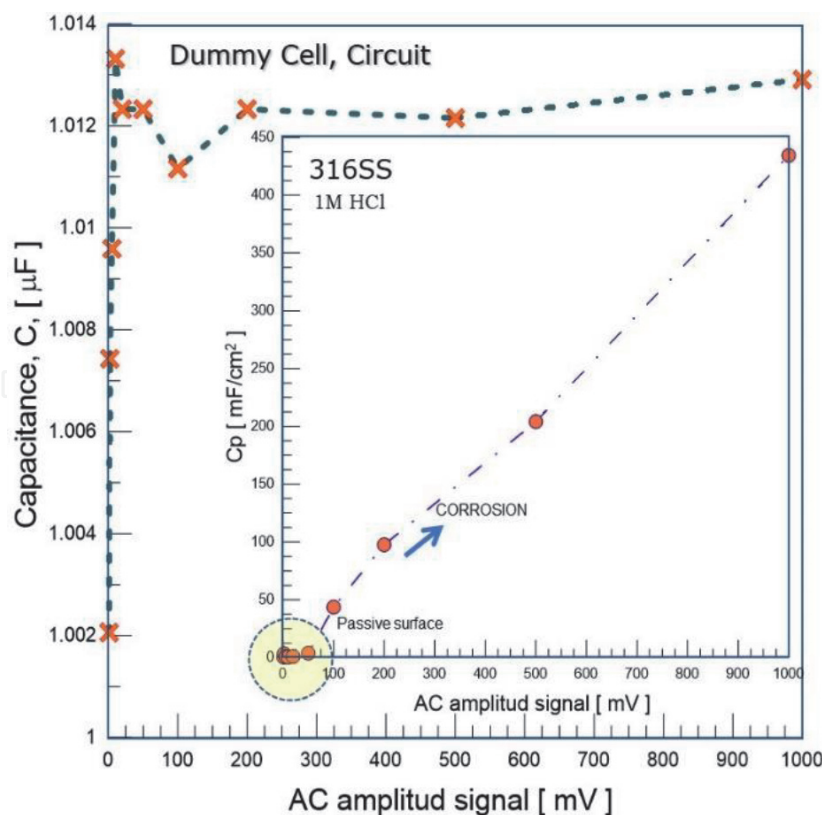


Figure 11.

AC amplitude signal dependence on capacitance value for an ideal EEC circuit model #1 ($C_1 = 1 \mu\text{F}$) and the stainless steel SS316 plate during its immersion in HCl 1 M.

film and manifestation of the pitting corrosion process that occurs after 200 mV, for this case an increase in the interface charge of electrons is expected with capacitances over 434.40 mF/cm^2 , like that as shown in **Figure 11**. It can conclude that it is possible to carry out experimental tests with amplitude signals ranging from 1 to 20 mV at the steady-state of corrosion potential without surface damage by the current applied, which is in according to the literature that reports an amplitude signal of 5 to 10 mv.

2.2 Kinetic oxidation reaction of steels tested in their received condition at different aqueous solutions

Figure 12 shows the typical impedance behavior of a steel with specification of AISI 8620 (0.20 wt.%C, 0.90 wt.%Mn, 0.35 wt.%Si, 0.60 wt.%Cr, 0.70 wt.%Ni, 0.25 wt.%Mo) in its received condition after exposed to different aqueous solutions such as distilled water, NaCl 0.5 M, HCl 1 M, H_2SO_4 1 M. The supplied voltage signal has an amplitude of 10 mV that fluctuating around the corrosion potential (-654 mV) in the frequency range of 1 MHz to 1 mHz, the response obtained is represented in Bode diagrams in which the impedance module and the phase angle serve as functions of the Log frequency, these diagrams indicate the sensitivity of the EIS technique to evaluate the presence of growth of a natural oxide on the steel surface, this is observed for the case of corrosion test in distilled water. Two well-defined time constants are observed in the evaluated frequency domain, one time constant at higher frequencies is related to the presence of an oxide layer, however, the intensity of the phase angle signal of 85° gives information about the oxide thickness and its adherence, however micro-cracks, closed porosity or growth defects are always present in many kinds of oxide layers that serve as conducting pathways of ions coming from the aqueous electrolyte, allowing electron charge

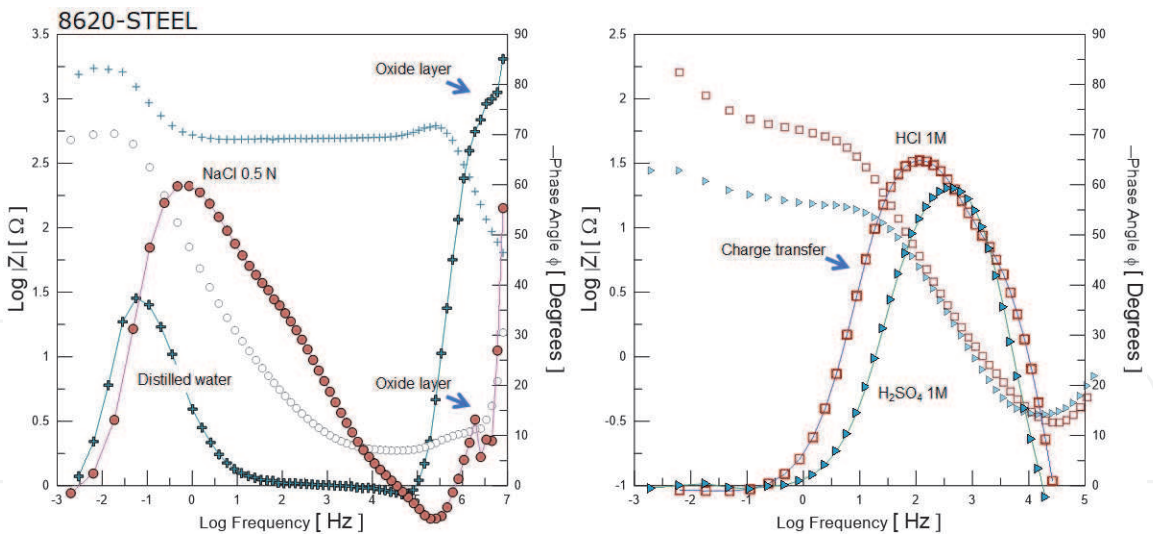


Figure 12.
Bode plots of impedance response of corroding 8620 plate at different aqueous solutions; distilled water, NaCl at 0.5 N, HCl at 1 M and H₂SO₄ at 1 M.

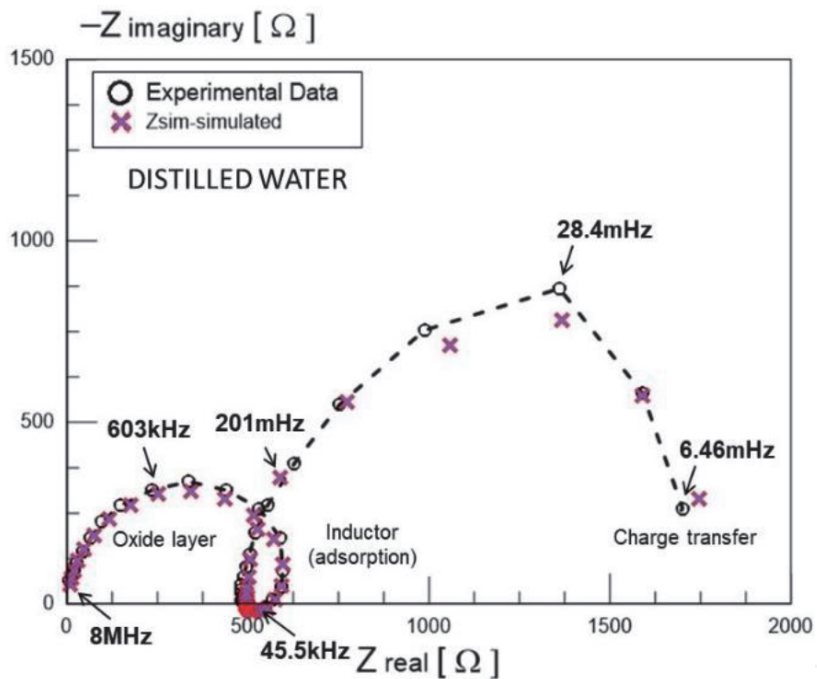


Figure 13.
Comparison of experimental and fitted EIS data for 8620 steel after exposure to distilled water.

transfer. This causes the phase-shifted continuously to zero degrees at frequencies between 80.7 kHz to 61.5 Hz, suggesting that the system behaves like a resistive component with a low flow of current near $10.3 \mu\text{A}/\text{cm}^2$, *i.e.* the current signal oscillates with the same phase as the potential does. In this frequency range an adsorptive process is carried out in which ions passing through the oxide layer defects, this mechanism is shown by the inductive response of the **Figure 13**. However, at lower frequencies over 8.59 Hz, an increase in the phase angle to 40° (56.6 mHz) is observed as if it were a capacitor in which the steel interface is charged by OH^- molecules, it is worth mentioning that this response is not related to the corrosion process, but this is a typical response to a passive system with a magnitude of impedance about $10^3 \Omega \cdot \text{cm}^2$.

On the other hand, when the pH of the aqueous solution decreases to an acidified stage by the presence of ions such as Na^+ , Cl^- , OH^- , SO_4^- , H^+ , the shape of the impedance diagrams has been change, for example, for NaCl solution, a slightly

acidified substance breaks-out almost the integrity of the natural oxide layer that covers the metal matrix and the response related to ion charge transfer to the metal interface is observed at lower frequencies. In addition to, an increase in current is also observed of about $34.479\text{ }\mu\text{A}/\text{cm}^2$ and a $|Z|$ of $10^2\Omega\text{-cm}^2$. Whereas, the same steel exposed to a more corrosive electrolyte such as HCl or H_2SO_4 at 1 M, the EIS response shows a single time constant that corresponding to the reaction's oxidation and reduction on the steel interface. That means, transient electrical charge events occur on the electrochemical double layer with ions, and is characterized by an increase of the current from 43.58 and $198.25\text{ }\mu\text{A}/\text{cm}^2$, respectively and the decrease of one order of magnitude of the impedance module $10^1\Omega\text{-cm}^2$, that is, less resistivity. The results in **Table 3** indicates the simulation of impedance parameters with an appropriate electrical circuit that have been describe before, these data suggest that a higher current passing and large electrical charging at the interface of the steel increases the susceptible to attack by corrosion, that is, the internal energy of the aqueous solution has the ability to degrade freely the steel by pitting corrosion.

Same behavior was observed for impedance-monitored corrosion tests for a 316 stainless steel plate (18.24 wt.%Cr, 8.07 wt.%Ni, 1.76 wt.%Mn, 0.5 wt.%Si, 0.27 wt.%Mo as principal alloying elements) after exposure to different aqueous solutions such as distilled water, 0.5 N NaCl, 0.5 N KCL, 1 M HCl or 0.5 M H_2SO_4 , **Table 4** shows the dissolution reaction. The impedance spectra that is shown in **Figure 14** indicates one of the advantages of the EIS technique to evaluate the performance of metal interface in full immersed to aggressiveness conditions of different electrolytes. In this sense the natural film of chromium oxide that protects stainless steel against corrosion is remarkable in distilled water by the presence of one time constant at higher frequencies with an impedance value near to $1\text{ M}\Omega\text{-cm}^2$.

Electrolyte	E_{corr} (mV)	I_{corr} ($\mu\text{A}/\text{cm}^2$)	C_{dl} ($\mu\text{F}/\text{cm}^2$)	R_{ct} ($\Omega\text{-cm}^2$)
Distilled water (circuit#5)	-654	10.3	21.01	1841.8
Sodium chloride, NaCl 0.5N (circuit#3)	-580	34.5	183.8	695.7
Hydrochloric acid, HCl 1M (circuit#1)	-438	43.5	379.5	61.5
Sulphuric acid, H_2SO_4 1M (circuit#1)	-489	194.3	515.2	15.0

Circuit #5

Circuit #3

Circuit #1

Table 3.
EIS parameters of simulated data to equivalent electrical circuit (EEC) for the steel 8620 during its exposure to different electrolytes.

Electrolyte	Concentration	C_{dl} ($\mu\text{F}/\text{cm}^2$)	Reaction
Distilled water	Pure-1lt	5.45	—
Sodium chloride, NaCl	29.2 gr/lt (0.5 N)	93.62	$\text{NaCl} + \text{H}_2\text{O} \rightarrow \text{Na}^+ + \text{Cl}^- + \text{OH}^-$
Potassium chloride, KCl	37.27 gr/lt (0.5 N)	165.3	$\text{KCl} + \text{H}_2\text{O} \rightarrow \text{K}^+ + \text{Cl}^- + \text{OH}^-$
Hydrochloric acid, HCl	15.56 ml/lt (1 M)	302.4	$\text{HCl} + \text{H}_2\text{O} \rightarrow \text{Cl}^- + \text{OH}^- + \text{H}_2\uparrow$
Sulfuric acid, H_2SO_4	27.11 ml/lt (1 M)	313	$\text{H}_2\text{SO}_4 + \text{H}_2\text{O} \rightarrow \text{SO}_4^- + \text{OH}^- + \text{H}_2\uparrow$

Table 4.
Capacitance of electrical double layer for the stainless steel SS316 during its exposure to different electrolytes.

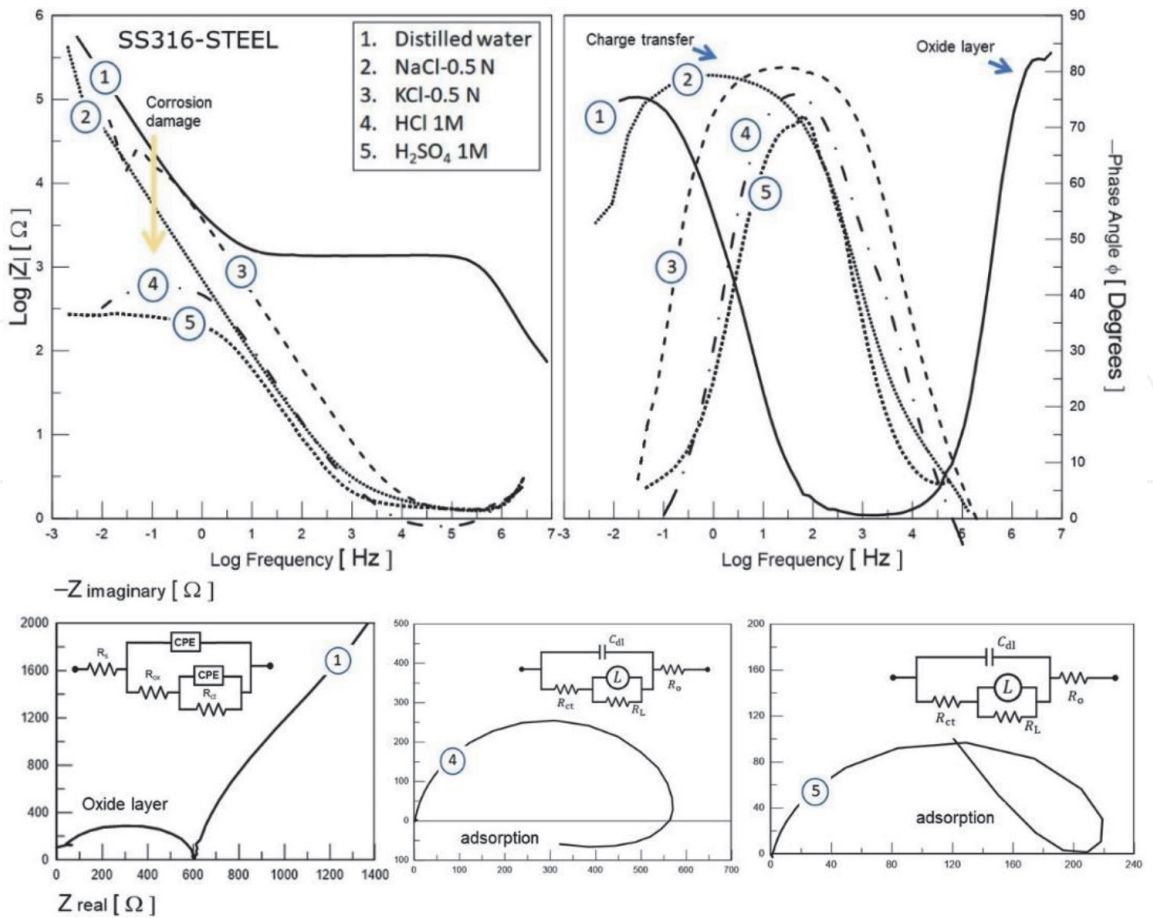


Figure 14.
Impedance response of corroding stainless steel (SS316) during exposure to (1) distilled water, (2) NaCl 0.5 N, (3) KCl 0.5 N, (4) HCl 1 M, and (5) H₂SO₄ 1 M.

Meanwhile, the presence of Cl⁻ ions (NaCl or KCl salt) alters the coating interface, which is electrically charged by ions causing the passivity state of stainless steel broken-down due to the dissolution of the oxide film, it is assumed that the steel is susceptible to corrosion by pitting. This is also seen through the presence of a time constant in the frequency domain studied. Similarly, the experimental tests in stronger acid media (HCl or H₂SO₄) indicate that stainless steel is seriously corroded in these conditions as a decrease in the impedance value below 1 mΩ-cm².

2.3 Steel corroded at non-stationary solution (rotating disk electrode, RDE condition)

Other application of the EIS technique is like that shown in **Figure 15**, which is the evaluation of the effect on hydrodynamic conditions on the corrosion process in steels. This particular study has an interest to show the behavior of a pipeline steel (API-5 L-X70) that is used for transportation of hydrocarbon fluid. This steel was immersed in HCl 1 M solution at a different rotation speed of the working electrode (WE) from 0 to 1500 rpm, *i.e.* from static conditions 0 rpm, laminar flow 1 to 200 rpm and to turbulent flow 300 to 1500 rpm. **Figure 15** shows the EIS response in the representation of Bode and Nyquist for the steel interface during its exposure to a corrosive media at different flow rates.

At the steady-state conditions, without rotation, the impedance response is related to electrons flow from the aqueous media to the metal interface allowing the formation of an interfacial layer over the metal surface, called an electrical double layer or a thin oxide film, which is indicated by the distortion of the semicircle

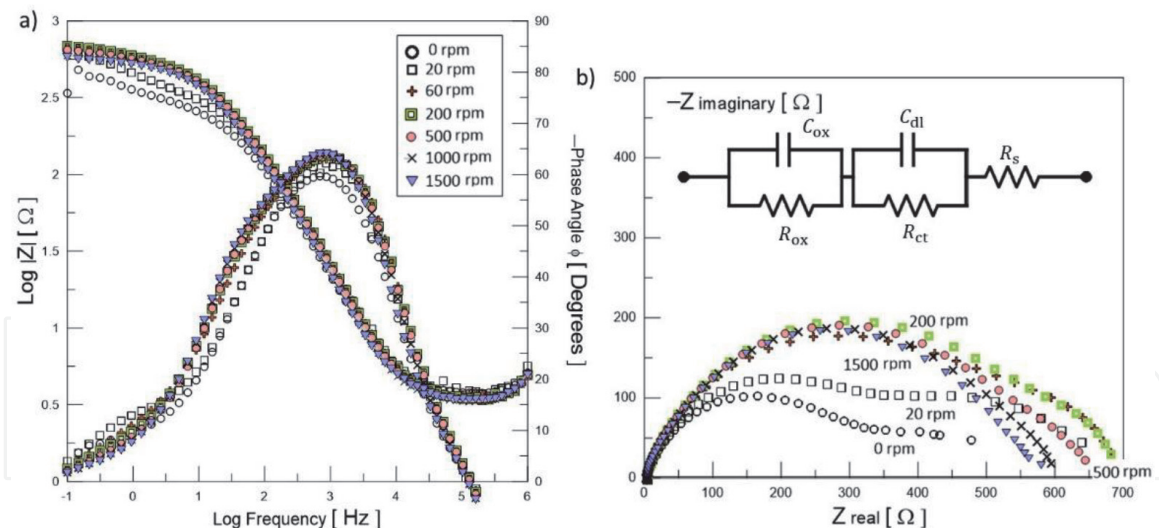


Figure 15.

Experimental impedance diagrams of corroding pipeline steel (API-5 L-X70) during exposure to HCl 1 M at different electrode rotation speed (0 to 1500 rpm). a) Bode plots representation and b) Nyquist complex plane.

presenting two time constants not very well-defined, besides in the diagram of bode two changes of slopes are shown for the impedance module. When applying rotation from 20 to 200 rpm an increase in the magnitude of the Z_{real} and Z_{imag} is observed due to the reaction kinetics at which the interfacial layer is forming at instantaneous rate and is controlled by electron charge and mass transfer mechanism. However, at turbulent conditions (>500 rpm) it does not allow the ions adsorption at the metal interface to maintain the presence of the double electrochemical layer or oxide film allowing only transients of electron transfer as a function of time, which promote the interfacial degradation of the steel. Therefore, the impedance diagrams show that under equilibrium conditions there is a corrosion rate controlled by the presence of a natural oxide on the steel surface, but this increased by the hydrodynamic conditions at turbulent flow, which is what is seen in real cases of application. But at moderate rotation speed the mass transport toward to the metal surface is carried out, giving opportunity to adsorption of molecules that come from the aqueous solution, which is consistent with the review literature [59].

2.4 Corrosion monitor in concrete reinforced materials

EIS technique can also be used for monitoring the evolution of the carbonation progress on concrete and the corrosion of the steel that serves as reinforcement. Carbonation results in a decrease in the pH of the cementation matrix when $\text{CO}_{2(g)}$ from the environment diffuses into the concrete structure, that can cause the loss of the passivity condition on the reinforcing steel surface and leads to an early failure of concrete by corrosion attack. Change in electrical resistance (R_{po}) and capacitance (C_{po}) of the concrete bulk is measured by a semicircle at high frequency region, which is the typical response of EIS diagram as that shown in **Figure 16**. More details are available in the research of H. Herrera in 2019 [6]. The corrosion test of this study was carried out on a fresh cross section of concrete sample after 7, 14, 21, 42, 61, 84, 106 and 120 days of artificially $\text{CO}_{2(g)}$ exposure periods (carbonation process). The characteristic impedance diagrams (EIS) of the concrete specimens after carbonation process at different ages of $\text{CO}_{2(g)}$ exposure during immersion in tap water are shown in **Figure 16**.

The EIS spectra is displayed in the Nyquist plots (Z_{real} vs. $Z_{\text{imaginary}}$), these results show a single capacitive well-defined semicircle at higher frequencies followed by a straight line for 7 to 84 days of carbonation, which indicates the

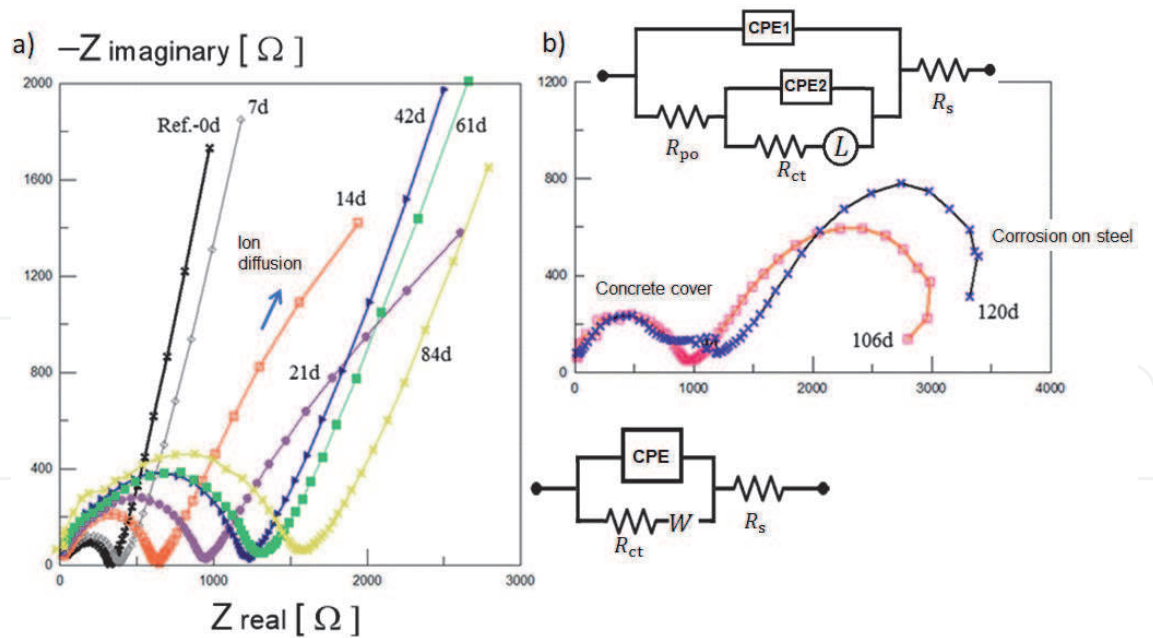


Figure 16.
EIS spectra for the particular system of concrete with reinforcing steel exposed to different days of a $CO_{2(g)}$ environment, carbonation process [6]. a) Nyquist complex plane showing the carbonation progress and b) Nyquist response for steel corroding.

specific resistance of the concrete that could be controlled by charge transfer process; while the straight line indicates a diffusion mechanism of ions through the pores. It is observed that the semicircle amplitude for the reference sample [REF.-0d, non-carbonated] is shorter than the carbonated samples at 7 or 120 days, this suggest that its resistance to the ions diffusion through the porous structure is much lower (a favorable condition for the ions coming from the aqueous solution driven easily into the porous structure of the concrete, resulting in the faster flow of electrons with chemical reactions and molecules adsorption processes around the vicinity of the steel interface), in addition to this, a typical signal describes a passive stage of the concrete. However, notable changes in the semicircle amplitude of the EIS spectra are observed, these changes are associated to the increase in electrical resistance (R) value of the concrete from 23.62 to 101.54 $k\Omega \cdot cm^2$ as the carbonation progress until to 84 days of $CO_{2(g)}$ exposure, this resulted to the blockade of the concrete pores by a calcium carbonate products, this reduces de alkalinity condition of the concrete matrix. However, the EIS diagrams for 106 days of exposure the resistance value decreases of about 58.26 $k\Omega \cdot cm^2$, the carbonation is almost complete, but after 120 days the resistivity still remains lower than 84 days of $CO_{2(g)}$ exposure (65.59 $k\Omega \cdot cm^2$) and the EIS spectra show remarkable changes in the low frequency domain. The changes registered by the EIS data for carbonated samples for 7 to 84 days are well-defined by one semicircle located at high frequencies (concrete porous resistance) with an infinite linear response at low frequencies (diffusion mechanism) only seen in the frequency domain of about $>10^6$ to 10^{-3} Hz by imposing a small amplitude of AC signal perturbation to the concrete/steel reinforcement system, this linear response was then modified by a second depressed semicircle with an inductive loop at lower frequencies in the domain of 10^{-6} Hz, using the EEC model #6 represents this behavior. The characteristic behavior of a second semicircle formed at lower frequencies for 106 or 120 days indicates that a process of corrosion may occur on the steel bar surface. The EIS parameters effectively demonstrate that after 106 days of exposure the carbonation is almost complete and corrosion damage is clearly progress on the steel bar. Carbonation progress was monitored by a significant increase in the diameter of the

semicircle, thus demonstrating the increase in resistivity of ions transmission due to blockade of pores by precipitation of CaCO_3 compounds. Finally, the *EIS* technique results a practical tool for evaluating the carbonation progress on reinforced concrete structures without causing structural damage, and its sensitivity to predict the activation of the reinforcing steel to be corroded.

2.5 Inhibition in organic molecules or natural liquids extracted from plants

Particularly, the Mexican's oil-industry still uses tubular steel pipes for the specific purpose of transporting hydrocarbons or natural gas. Most of the lines are buried, so the national network extends over quite large distances, crossing varied terrains conditions some with rivers, others with salt-laden marshes, or polluted industrial or urban zones alike; the ambient temperatures and load pressure for the buried-pipelines network vary widely, to put it simply vulnerable to corrosion attack. Steel pipes are corroded as a result of iron oxidation during its exposure of longer service periods. Therefore, corrosion problems are directly related to ever-present economical and production losses, as well as environment affectations, though human losses also happen. Providing effective inhibiting substances that are added to processing fluids may reduce internal corrosion problems; there are a wide variety of organic substances known to act as corrosion inhibitors. **Figure 16** have demonstrated that small inhibitor quantities of organic molecules (2-Mercaptobenzimidazole, *MBI* or 5-Nitro-2-Mercaptobenzimidazole *NMBI*) can be added to the media to diminish its inherent aggressiveness toward the steel surfaces [18, 60, 61]. It becomes evident that testing with the largest *2MBI* concentration, namely 200 ppm, there began to appear two-time constants, which suggests that two different processes are involved during the perturbation. One is related to a molecular adsorption mechanism of the organic compound over the polished metal surface, thus giving rise to multilayers, while the second constant is related to infiltration of the corrosive species through assorted passages formed during self-assembly and rearrangement of the organic molecules, very probably due to the diversity of interactive forces operating on the electrode system. This second time constant that operates at intermediate frequencies can be interpreted as a resistance to charge transfer. The *2MBI* inhibitor gave inhibiting efficiencies over 96% after adding only 20 ppm covering the metal surface exposed to the acid medium 1 M HCl. Therefore, the heterocyclic organic molecule *2MBI* was an efficient inhibitor in H_2SO_4 at 25 ppm. The plot of $\log Z$ vs. $\log f$, shown in **Figure 17**, reveals that as the inhibitor concentration increases, so does the impedance, which is also related to the charge transfer resistance, R_{ct} . This value was obtained through fitting a *RC* electrical circuit model #3 to the experimental data. The $|Z|$ increment is explained by the excess of inhibitor's molecules in the solution, which as being bipolar it tends to adhere to the metal surface, also interacting among them thus forming a multilayered assembly, capable of blocking the electron charge transfer, refer to **Figure 17**, to appreciate more clearly the said $|Z|$ increase.

Furthermore, Natural liquid-extracts like *Morinda citrifolia* has been used as corrosion inhibitor for steels (AISI-1045) exposed to acidic environments of HCl. Both the organic and inorganic compounds commonly used in the industry to inhibit the corrosion process of metals and its alloys are mostly composed by highly toxic chemicals, in addition to being more expensive. In this research sugar-components derived from the *Morinda citrifolia* (MC) leaves have been extracted in aqueous solutions to perform a natural inhibitor capable to control de corrosion damage, which can replace the traditional inhibitors, being environmentally friendly [62, 63]. The experimental results indicate that this compound has shown excellent performance as corrosion inhibitor, reaching inhibition efficiency (*EI*),

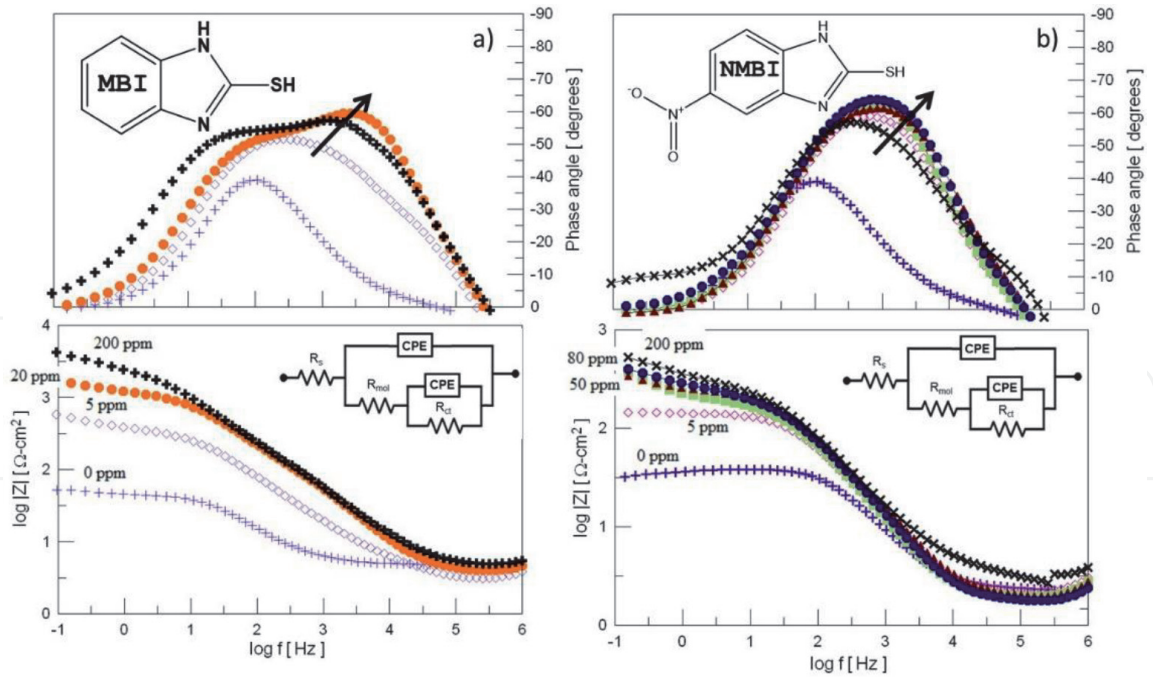


Figure 17.
EIS spectra in bode plots obtained from the pipeline steel API-5 L-X52 samples immersed in H_2SO_4 1 M as a function of the 2MBI or 5NMBI at different concentration [60, 61]. a) Response for 2- Mercaptobenzimidazole and b) response for 5-Nitro-2-Mercaptobenzimidazole.

values up to 90% at inhibitor concentrations ranging 0.8 to 2 g/L and immersion times of about 1 to 4 h. It has been found that the inhibition process takes place by the adsorption of the molecules on the surface of the metal (AISI 1045), by a physisorption mechanism. See **Figure 18**.

2.6 Hard-coatings as protection; borided treatment

Other attractive uses of the *EIS* technique are its application to evaluate the integrity and coating performance during its exposure in corrosive environments as a function of time. Actually, *EIS* is used as a quality control to evaluate the process

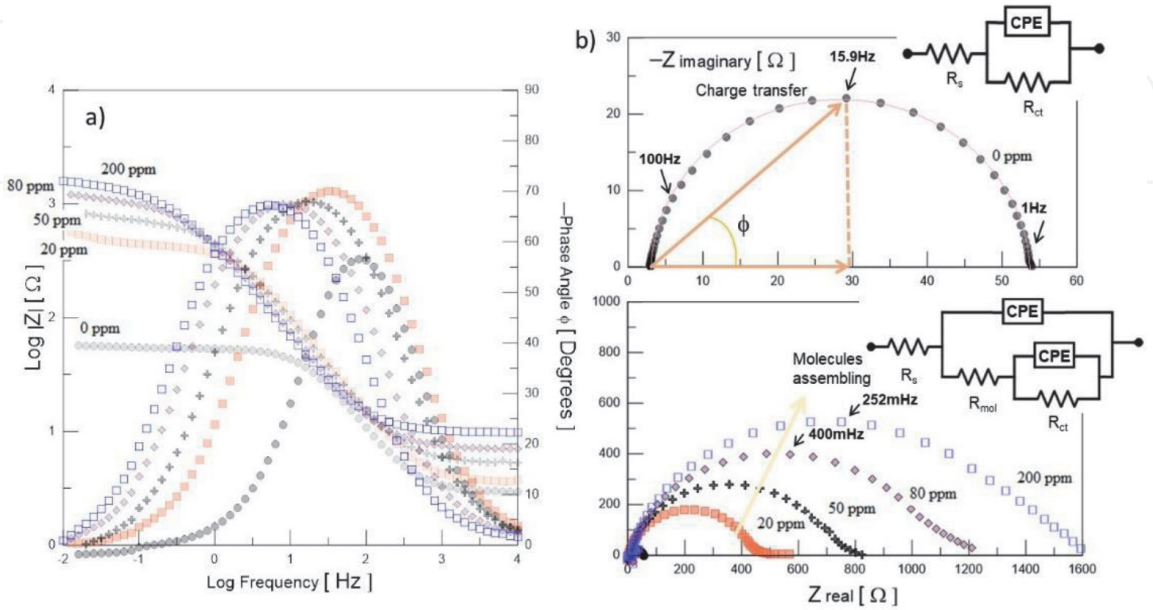


Figure 18.
EIS spectra in bode plots obtained from the pipeline steel API-5 L-X52 samples immersed in H_2SO_4 1 M as a function of the different concentration of natural molecules.

of surface finishing treatments in many industries. In this sense, the results of **Figure 19** show the characteristic impedance spectra that indicate the quality properties and corrosion resistance of a $\text{Fe}_2\text{B}/\text{FeB}$ hard coating formed by boron atomic diffusion on the steel surface of a 1045 and 304 stainless steel during the boriding thermochemical treatment. Boriding is recognized as a thermochemical surface treatment in which boron diffuses into the ferrous substrate and reacts with Fe atoms of the bulk material to form a single (Fe_2B) or double-phase ($\text{Fe}_2\text{B}/\text{FeB}$) layer with a well-defined thickness and composition [14]. The thickness of each layer has considerable effects on the mechanical behavior and corrosion behavior of the borided steels. However, the quality of the hard boride coatings depends essentially on the boriding temperature, treatment time, chemical composition of the steel substrate and the amount of boron atoms available around the sample surface to be coated.

In this study, in particular a powder-pack boriding was used on AISI-SAE 1045 steel and SS316 stainless steel as surface thermochemical treatment to improve hardness and wear resistance to the steel samples, due to its low cost of hard coating processing. Boriding can also enhance the corrosion resistance of ferrous materials as shown in **Figure 19**. The results indicate that a single boride layer of Fe_2B is

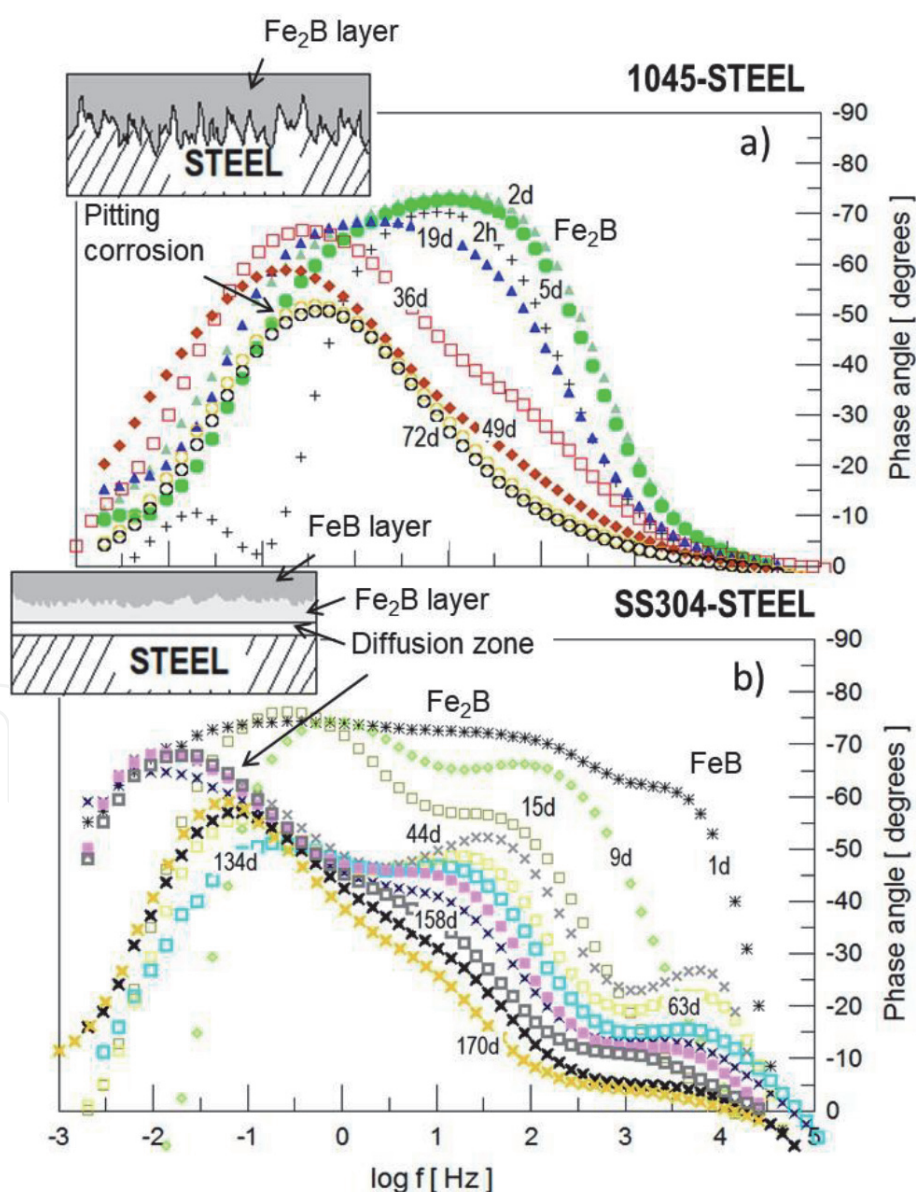


Figure 19.

EIS spectra for borided samples immersed in HCl 1 M as a function on exposure time. Boriding treatment was performed on AISI 1045 steel or AISI SS304 stainless steel treated at 950°C for 6 h [14]. a) Phase angle response for borided 1045 steel and b) Phase angle dependence for borided SS304 steel.

formed on the 1045 steel surface, its morphology consisting a deep saw-tooth derived from the existence of diffusion paths (porosity and micro-cracks) in the surface of the steel matrix, in which the boron atoms are interstitial inserted to the surface forming a stable phase. For the borided stainless steel SS304 at the same conditions forms two-well defined layers on the surface, the columnar phase that was growth on the 1045 steel is less intense for SS304, this is due to the high concentration of chromium and nickel on the substrate surface, so the diffusion of boron stops by reacting immediately to form interstitial compounds of CrB, Cr₂B or Ni₃B in combination with FeB and Fe₂B. EIS for the borided 1045 steel were recorded over 72 days of exposure to HCl 1 M solution, which the hard coating degrades slowly due to the defects on the coating structure that allow Cl⁻ ions infiltrate, this is denote by changing the *EIS* spectra shape from one time constant to two time constant with a clearly phase-angle shifted and loss of impedance value, that means pitting corrosion initiation. No-corrosion damage was observed for the borided SS304 during its exposure in HCl 1 M solution for at least 170 days. Three times constants were observed after 44 days that's reveal the presence of the FeB layer, after Fe₂B layer and the diffusion layer.

2.7 Steels used as beverages container

Steel-can containers are manufactured from thin metal plates and are commonly used for the distribution or storage of food or beverages. Most conventional steel beverage cans have bent to form a tube and then welding both sides leaving a firm seam, then joining the bottom end to the tube, finally, the steel can is filling-out with the content. However, it is necessary to mention that the steels cans have an internal polymer coating or have been treated by electroplating to coated internally with a thin layer of tin in order to prevent any oxidizing or electrochemical corrosion during the steel exposure to the liquid product that it contains, which could be carbonated soft drinks, alcoholic drinks, fruit juices, teas, herbal teas, energy drinks and others [64, 65]. Despite of this internal coating having the good quality, it may fracture during storage or dissolve in small amounts in the liquid product, which depends on certain factors such as temperature, stowage load and handling of the products during their storage, as well as the chemical composition of the liquid and steel. Due to this, efforts have been managed to replace tin-based coatings by chemical compounds derived from epoxy resins or polymers. Nevertheless, the set-up of the factors mention above may situate the metal container (e.g. steel cans) at a potential risk to develop internal corrosion.

On the other hand, the sale of beverages storage in steel cans are committed to their handling in warehouse, in this way, there is a predisposition of the people who buy drink-cans, they think if cans are struck or bent the coating has been damaged and could be associated that the liquid product is contaminated with Fe⁺ ions. The impedance diagrams of **Figure 20** show that the *EIS* technique can be applied to assess the corrosion resistance of the internal coating in a specific beverage can.

In this case experimental corrosion tests on laboratory conditions were performed in a metal container used for the distribution of orange juice in Mexico. This can is made of steel with internally coated by a higher density polymer. Three particular cases are studied as denoted in the scheme of **Figure 20**; *EIS* spectra shown the behavior for a) with the coating, b) when the coating is mechanically damaged by a scratch and c) absence of coating, measured in HCl 1 M as a function of AC amplitude signal from 5 to 1000 mV. The bode diagrams indicate the presence of two well-defined time constants in the entire frequency domain for 5 and 10 mV of signal, the first one is related to the polymer coating with a resistance of electron -ion transfer of about 10⁸Ω -cm² with a micro-porous net (conducting paths) inside the coating as indicated by the second time constant. However as increasing the amplitude of signal

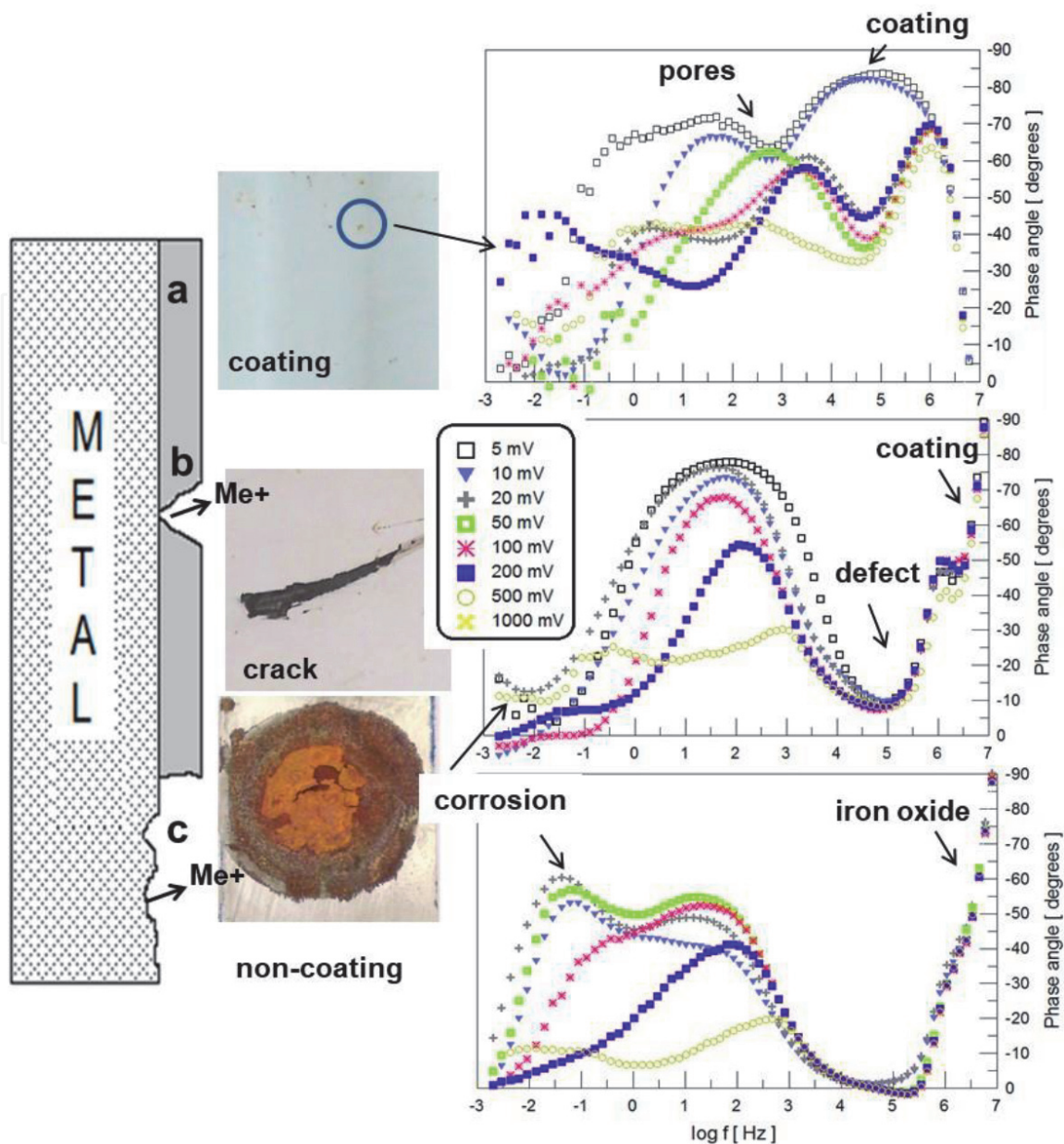


Figure 20.

Phase angle EIS response obtained for metal beverage containers at different surface condition after immersed in NaCl 0.5 M as a function on AC amplitude signal. a) Uniform polymer coating, b) scratch defect on coating, c) polished surface no-coating.

voltage the $|Z|$ value drops below $10^4 \Omega\text{-cm}^2$, this response is associated with local stain-spots on the coating, which is indicted by a third time constant a low frequency. In the condition for the coating damaged by a localized defect such as a scratch or fracture, the impedance value decreases severely to 10^5 to $10^2 \Omega\text{-cm}^2$ as increased the AC signal, one time constant indicates the electron charge transfer processes through the defect that cause ions to be diffused below the coating until its failure. Finally, for the condition in the absence of the coating on the steel plate, the impedance diagrams show the corrosion process of the steel at different AC signal amplitudes, which shows severe corrosion after 200 mV showing $10^1 \Omega\text{-cm}^2$ of $|Z|$ value.

3. Conclusions

This review study is related to the basic aspects of EIS to understand the corrosion mechanism of industrial steels that serve at different corrosive conditions,

which has a great interest on giving an educational orientation and practical teaching guide of how to use the outstanding Electrochemical Impedance Spectroscopy (EIS) technique in metal corrosion technology. Therefore, this review considers a wide variety of practical electrochemical impedance cases based on the fundamental and qualities aspects of EIS theory and its experimental interpretation. This book chapter also serves as a support for postgraduate students to have a criterion in deciding through their own experiences when using the electrochemical impedance technique. The practical cases discussed here are part of the research experienced of Dr. Héctor Herrera Hernández (DR.3H) and his students & research group. It is worth to mention that EIS has been extended to various disciplines of science and technology, thus demonstrating great efficiency in evaluating the performance and integrity of metallic materials as can be seen in detail in the practical examples presented in this review work. So, EIS is not only applied to stationary conditions, but also more complex variables can be monitored such as: flow parameters, variable that undoubtedly represents the real conditions and could be an interesting challenge for analyzing and interpreting these phenomena by means of EIS data. The fitting EIS data using a mathematical model such as an equivalent electrical circuit is a critical process in the analysis and validation of EIS data for the acquisition of the system's electrical parameters that can be related to the corrosion rate of the material under study and also gives information of its capacity of electrons charge. Finally, EIS seeks to obtain information on the system and its evolution with time by applying a sinusoidal voltage as a function of frequency range, in order to determine the properties and feasibility of materials that serve under severe service conditions, such as industrial steels as is this case of the reviewed book chapter.

Acknowledgements

The authors dedicate this chapter to the memory of Professor Florian B. Mansfeld, USC.

The authors would like to acknowledge and express their gratitude to CONACyT for the SNI distinction as research membership and the monthly stipend received. Héctor Herrera Hernández (DR.3H) also would like to thanks to CIDETEQ and Secretaria de Investigación y Estudios Avanzados SIyEA/UAEM for their financial support through research project (4602/2018E). This project was conducted in the (Laboratory of Electrochemical and Corrosion of Industrial Materials at UAEM). Finally, DR.3H dedicates this work in memory to Professor **Florian B. Mansfeld**, for his teaching and guidance in the way of science (EIS technique), FBM will be remembered forever for his outstanding knowledge and contributions.

IntechOpen

Author details

Héctor Herrera Hernández^{1*}, Adriana M. Ruiz Reynoso¹,
Juan C. Trinidad González¹, Carlos O. González Morán¹,
José G. Miranda Hernández¹, Araceli Mandujano Ruiz², Jorge Morales Hernández²
and Ricardo Orozco Cruz³


1 Laboratorio de Investigación en Electroquímica y Corrosión de Materiales Industriales, Universidad Autónoma del Estado de México, Blvd. Universitario s/n, Predio San Javier Atizapán de Zaragoza, Estado de México 54500, México

2 Centro de Investigación y Desarrollo Tecnológico en Electroquímica, S.C., Parque Tecnológico Querétaro s/n, Sanfandila, Querétaro 76703, México

3 Instituto de Ingeniería, Universidad Veracruzana, S.S. Juan Pablo II s/n. Col., Zona Universitaria, Boca del Río, Veracruz 94294, México

*Address all correspondence to DR.3H: hherrerah@uaemex.mx

IntechOpen

© 2020 The Author(s). Licensee IntechOpen. This chapter is distributed under the terms of the Creative Commons Attribution License (<http://creativecommons.org/licenses/by/3.0>), which permits unrestricted use, distribution, and reproduction in any medium, provided the original work is properly cited. 

References

- [1] Marcus P, Oudar J. Corrosion Mechanism in Theory and Practice. 1st ed. New York: Marcel Dekker, Inc.; 1995. 641p. DOI: 10.1201/9780203909188
- [2] American Society for Metals. ASM Handbook, Vol. 13A Corrosion: Fundamentals, Testing and Protection. 10th ed. Ohio: ASM International; 2003. 2597p. DOI: 10.31399/asm.hb.v13b.9781627081832.
- [3] Morcillo M, De la Fuente D, Díaz I, Cano H. Atmospheric corrosion of mild steel. *Revista de Metalurgia*. 2011;47(5): 1-19. DOI: 10.3989/revmetalm.1125
- [4] Corrosion LD. Surface Chemistry of Metals. 1st ed. Vol. 614p. Florida: Taylor and Francis Group; 2007. DOI: 10.1201/9781439807880.
- [5] Ahmad Z. Principles of Corrosion Engineering and Corrosion Control. 1st ed. Vol. 656p. Oxford: Butterworth-Heinemann; 2006. DOI: 10.1016/B978-0-7506-5924-6.X5000-4.
- [6] Herrera Hernández H, González Díaz F, Fajardo SanMiguel G, Velázquez Altamirano JC, González Morán CO, Morales Hernández J. Electrochemical impedance spectroscopy as a practical tool for monitoring the carbonation process on reinforced concrete structures. *Arabian Journal for Science and Engineering*. 2019;44:10087-10103. DOI: 10.1007/s13369-019-04041-z
- [7] Khatak HS, Raj B. Corrosion of Austenitic Stainless Steels. 1st ed. Alpha Science International: Pangbourne; 2002. 400p. DOI: 10.1002/maco.200490073
- [8] Kelly RG, Scully JR, Shoesmith DW, Buchheit RG. Electrochemical Techniques in Corrosion Science and Engineering. 1st ed. New York: Marcel Dekker Incorporation; 2002. 440p. DOI: 10.1201/9780203909133
- [9] Garfias-Garcia E, Colin-Paniagua FA, Herrera-Hernandez H, Juarez-Garcia JM, Palomar-Pardavé ME, Romero-Romo MA. Electrochemical and microscopy study of localized Corrosion on a sensitized stainless steel AISI 304. *ECS Transactions*. 2010;29(1):93-102
- [10] Outokumpu. Handbook of stainless steel. 1st ed. Avesta: Outokumpu Oyj; 2013. 92p.
- [11] Liang W. Surface modification of AISI 304 austenitic stainless steel by plasma nitriding. *Applied Surface Science*. 2003;211:308-314. DOI: 10.1016/S0169-4332(03)00260-5
- [12] Liu RL, Yan MF. Improvement of wear and corrosion resistances of 17-4PH stainless steel by plasma nitrocarburizing. *Materials and Design*. 2010;31:2355-2359. DOI: 10.1016/j.matdes.2009.11.069
- [13] Cardoso RP, Mafra M, Brunatto SF. Low-temperature thermochemical treatments of stainless steels. In: Mieno T, editor. *Plasma Science and Technology: Progress in Physical States and Chemical Reactions*. 1st ed. London: IntechOpen; 2016. pp. 107-130. DOI: 10.5772/61989
- [14] Mejia-Caballero I, Martínez-Trinidad J, Palomar-Pardavé M, Romero-Romo M, Herrera-Hernández H, Herrera-Soria O, et al. Electrochemical evaluation of corrosion on borided and non-borided steels immersed in 1M HCl solution. *Journal of Materials Engineering and Performance*. 2014;23:2809-2818. DOI: 10.1007/s11665-014-1039-z
- [15] Martini C, Palombarini G, Carbucicchio M. Mechanism of thermochemical growth of iron borides on iron. *Journal of Materials Science*. 2004;39:933-937. DOI: 10.1023/B:JMSC.0000012924.74578.87

- [16] Natalya V. Likhanova NV, Domínguez-Aguilar MA, Olivares-Xometl O, Nava-Entzana N, Arce E, Dorantes H. The effect of ionic liquids with imidazolium and pyridinium cations on the corrosion inhibition of mild steel in acidic environment. *Corrosion Science*. 2010;52:2088–2097. DOI: 0.1016/j.corsci.2010.02.030.
- [17] Goyal M, Kumar S, Bahadur I, Verma C, Ebenso EE. Organic corrosion inhibitors for industrial cleaning of ferrous and non-ferrous metals in acidic solutions: A review. *Journal of Molecular Liquids*. 2018;256:565-573. DOI: 10.1016/j.molliq.2018.02.045
- [18] Abreu-Quijano M, Palomar-Pardavé M, Cuán A, Romero-Romo M, Negrón-Silva G, Álvarez-Bustamante R, et al. Quantum chemical study of 2-Mercaptoimidazole, 2-Mercaptobenzimidazole, 2-Mercapto-5-Methylbenzimidazole and 2-Mercapto-5-Nitrobenzimidazole as Corrosion inhibitors for steel. *International Journal of Electrochemical Science*. 2011;6: 3729-3742
- [19] Krim O, Elidrissi A, Hammouti B, Ouslim A, Benkaddour M. Synthesis, characterization, and comparative study of pyridine relatives as corrosion inhibitors of mild steel in HCl medium. *Chemical Engineering Communications*. 2009;196(12):1536-1546. DOI: 10.1080/00986440903155451
- [20] Palomar-Pardavé M, Romero-Romo M, Herrera-Hernández H, Abreu-Quijano MA, Likhanova NV, Uruchurtu J, et al. Influence of the alkyl chain length of 2-amino 5-alkyl 1,3,4-thiadiazole compounds on the corrosion inhibition of steel immersed in sulfuric acid solutions. *Corrosion Science*. 2012; 54:231-243. DOI: 10.1016/j.corsci.2011.09.020
- [21] Singh AK, Quraishi MA. The effect of some bis-thiadiazole derivatives on the corrosion of mild steel in hydrochloric acid. *Corrosion Science*. 2010;52(4):1373-1385. DOI: 10.1016/j.corsci.2010.01.007
- [22] Bouklah M, Ouassini A, Hammouti B, Idrissi AE. Corrosion inhibition of steel in sulphuric acid by pyrrolidine derivatives. *Applied Surface Science*. 2006;252:2178-2185
- [23] Ansari K, Yadav DK, Ebenso EE, Quraishi M. Novel and effective pyridyl substituted 1, 2, 4-triazole as corrosion inhibitor for mild steel in acid solution. *International Journal of Electrochemical Science*. 2012;7:4780-4799. DOI: : 10.1016/j.corsci.2011.09.020.
- [24] Espinoza-Vázquez A, Negrón-Silva GE, González-Olvera R, Angeles-Beltrán D, Herrera-Hernández H, Romero-Romo M, et al. Mild steel corrosion inhibition in HCl by di-alkyl and di-1, 2, 3-triazole derivatives of uracil and thymine. *Materials Chemistry and Physics*. 2014;145: 407-417. DOI: 10.1016/j.matchemphys. 2014.02.029
- [25] Mansfeld F. Don't Be afraid of electrochemical techniques — But use them with care. *Corrosion Science*. 1988;44(12):856-868. DOI: 10.5006/1.3584957.
- [26] Bard JA, Methods FRLE. Fundamentals and applications. John Wiley & Sons, Inc. 2nd. In: USA. 2001
- [27] Mansfeld F, Lee CC, Zhang G. Comparison of electrochemical impedance and noise data in the frequency domain. *Electrochimica Acta*. 1998;43(3–4):435-438. DOI: 10.1016/s0013-4686(97)00060-1
- [28] Mansfeld F, Lee CC, Zhang G. Comparison of electrochemical Impedance and noise data for polymer coated steel in the frequency domain. *Materials Science Forum*. 1998;289-292: 93-106. DOI: 10.4028/www.scientific.net/msf.289-292.93

- [29] Mansfeld F. Use of electrochemical impedance spectroscopy for the study of corrosion protection by polymer coatings. *Journal of Applied Electrochemistry*. 1995;25(3):187-202. DOI: 10.1007/bf00262955
- [30] Mansfeld F. Electrochemical impedance spectroscopy (EIS) as a new tool for investigating methods of corrosion protection. *Electrochimica Acta*. 1990;35(10):1533-1544. DOI: 10.1016/0013-4686(90)80007-b
- [31] Mansfeld F, Xiao H, Wang Y. Evaluation of localized corrosion phenomena with electrochemical impedance spectroscopy (EIS) and electrochemical noise analysis (ANA). *Materials and Corrosion*. 1995; 46(1):3-12. DOI: 10.1002/maco.19950460103
- [32] Bolind AM, Lillard RS, Subbina JF. The electrical AC impedance response of oxide scales on 9Cr-1Mo steel immersed in molten lead-bismuth eutectic alloy at 200°C. *Corrosion Science*. 2015;92:48-57. DOI: 10.1016/j.corsci.2015.11.012.
- [33] Shih H, Mansfeld F. A fitting procedure for impedance data of systems with very low corrosion rates. *Corrosion Science*. 1989;29(10): 1235-1240. DOI: 10.1016/0010-938X(89)90070-X
- [34] Macdonald DD. Why electrochemical impedance spectroscopy is the ultimate tool in mechanistic analysis. *ECS Transactions*. 2009;19(20):55-79
- [35] González-Morán CO, Miranda-Hernández JG, Flores Cuautle JJA, Suaste-Gómez E, Herrera-Hernández H. A PLZT novel sensor with Pt implanted for biomedical application: Cardiac micropulses detection on human skin. *Advances in Materials Science and Engineering*. 2017;2017:1-7. DOI: 10.1155/2017/2054940
- [36] Macdonald DD. A method for estimating Impedance parameters for electrochemical systems that exhibit Pseudoinductance. *Journal Electrochemical Society*. 1978;125(12): 2062-2064
- [37] Barsoukov E, Macdonald J.R. *Impedance Spectroscopy theory, experiment, and applications*. 2nd ed. Hoboken: A John Wiley & Sons Incorporation; 2005. 595p.
- [38] Lvovich VF. *Impedance Spectroscopy: Applications to Electrochemical and Dielectric Phenomena*. 1st ed. Hoboken: A John Wiley & Sons Incorporation; 2012 353p
- [39] Electrical Impedance CL. *Principle, measurement, and applications*. 1st ed. broken Sound Parkway: Taylor & Francis. Group. 2013;279p
- [40] Dalmont JP. Acoustic Impedance measurement, part I: A review. *Journal of Sound and Vibration*. 2001;243(3): 427-439. DOI: 10.1006/jsvi.2000.3428
- [41] Alberts B, Johnson A, Lewis J, Raff M, Roberts K, Walter P. *Molecular biology of the cell*. 4th ed. Totnes: Garland. Science. 2002;3786p
- [42] Gamry Instruments. Basics of Electrochemical Impedance Spectroscopy [Internet]. 2020. Available from: [http:// www.gamry.com/application-notes/EIS/basics-of-electrochemical-impedance-spectroscopy/.html](http://www.gamry.com/application-notes/EIS/basics-of-electrochemical-impedance-spectroscopy/.html) [Accessed: 2020-08-23]
- [43] Perez N. *Electrochemistry and Corrosion Science*. 1st ed. Vol. 362p. New York: Kluwer Academic Publishers; 2004
- [44] Mendoza-Flores J, Durán-Romero R, Genescá-Llongueras J. Espectroscopía de Impedancia Electroquímica en Corrosión. In: Llongueras JG, editor. *Notas Técnicas Electroquímicas para el control y estudios de la corrosión*. México: UNAM. 2002. pp. 55-91

- [45] Mansfeld F, Shih h, Greene H, Tsai CH. Analysis of EIS data for common corrosion processes. In: Scully JR, Silverman DC, Kendig MW, editors. *Electrochemical Impedance: Analysis and Interpretation*. 1st ed. Fredericksburg: ASTM publication; 1993. pp. 37-53
- [46] Mandujano-Ruiz A, Corona-Almazán E, Herrera-Hernández H, Morales-Hernández J. Opuntia ficus-indica (Nopal extract) as green inhibitor for Corrosion protection in industrial steels. In: Aliofkhazraei M, editor. *Corrosion Inhibitors, Principles and Recent Applications*. Croacia: Intech; 2018. pp. 145-158. DOI: 10.5772/intechopen.72944
- [47] Hsu CH, Mansfeld F. Technical note: Concerning the conversion of the constant phase element parameter Y_0 into a capacitance. *Corrosion*. 2001; **57**(9):747-748. DOI: 10.5006/1.3280607
- [48] Urquidi-Macdonald M, Real S, Macdonald DD. Applications of Kramers—Kronig transforms in the analysis of electrochemical impedance data—III. Stability and linearity. *Electrochimica Acta*. 1990;**35**(10): 1559-1566. DOI: 10.1016/0013-4686(90)80010-1
- [49] Matthew J, Orazem ME. On the application of the Kramers-Kronig relations to evaluate the consistency of electrochemical Impedance data. *Journal Electrochemical Society*. 1991; **138**:67-75
- [50] Mansfeld F. Electrochemical impedance spectroscopy (EIS) as a new tool for investigating methods of corrosion protection. *Electrochimica Acta*. 1990;**35**(10):1533-1544. DOI: 10.1016/0013-4686(90)80007-b
- [51] Mansfeld F, Kendig MW. Electrochemical Impedance spectroscopy of protective coatings. *Materials and Corrosion*. 1985;**36**(11): 473-483. DOI: 10.1002/maco.19850361102
- [52] Mansfeld F, Tsai CH. Determination of coating deterioration with EIS: I. basic relationships. *Corrosion*. 1991;**47**(12): 958-963. DOI: 10.5006/1.3585209
- [53] Tsai CH, Mansfeld F. Determination of coating deterioration with EIS: Part II. Development of a method for field testing of protective coatings. *Corrosion*. 1993;**49**(9):726-737. DOI: 10.5006/1.3316106
- [54] Song YK, Mansfeld F. Development of a molybdate–phosphate–silane–silicate (MPSS) coating process for electrogalvanized steel. *Corrosion Science*. 2006;**48**(1):154-164. DOI: 10.1016/j.corsci.2004.11.028
- [55] Amirudin A, Thierry D. Application of electrochemical impedance spectroscopy to study the degradation of polymer-coated metals. *Progress in Organic Coatings*. 1995;**26**:1-28. DOI: 10.1016/0300-9440(95)00581-1
- [56] Yao Z, Jiang Z, Wang F. Study on corrosion resistance and roughness of micro-plasma oxidation ceramic coatings on Ti alloy by EIS technique. *Electrochimica Acta*. 2007;**52**(13): 4539-4546. DOI: 10.1016/j.electacta.2006.12.052
- [57] Bosch RW, Moons F, Zheng JH, Bogaerts WF. Application of electrochemical Impedance spectroscopy for monitoring stress Corrosion cracking. *Corrosion Science*. 2001;**57**(6):532-539. DOI: 10.5006/1.3290379
- [58] Gómez-García J, Rico A, Garrido-Maneiro MA, Múnez CJ, Poza P, Utrilla V. Correlation of mechanical properties and electrochemical impedance spectroscopy analysis of thermal coatings. *Surface & Coatings Technology*. 2009:812-815. DOI: 10.1016/j.surfcoat.2009.09.064

- [59] Espinoza-Vázquez A, Negrón-Silva GE, Angeles-Beltrán D, Herrera-Hernández H, Romero-Romo M, Palomar-Pardavé MNEIS. Evaluation of pantoprazole as Corrosion inhibitor for mild steel immersed In HCl 1 M. effect of [pantoprazole], hydrodynamic conditions, temperature and immersion times. *International Journal of Electrochemical Science*. 2014;**9**: 493-509
- [60] Espinoza A, Negrón G, Palomar-Pardavé ME, Romero-Romo MA, Rodríguez I, Herrera-Hernández H. Electrochemical Impedance spectroscopy analysis of 2-Mercaptobenzimidazole (2MBI) as Corrosion inhibitor in HCl 1M. *ECS Transactions*. 2009;**20**(1):543-553. DOI: 10.1149/1.326842.
- [61] Cruz DY, Negrón G, Romero-Romo MA, Herrera-Hernández H, Palomar-Pardavé ME. Microwave-assisted preparation of 2-(Benzylthio)imidazole and 2-(Benzylthio)benzimidazole and its comparative Corrosion inhibiting performance with 2-Mercaptoimidazole and 2-Mercaptobenzimidazole. *ECS Transactions*. 2009;**20**(1):519-527. DOI: 10.1149/1.3268419.
- [62] Barreto E. Extractos líquidos naturales de Morinda Citrofolia y Aloe-Vera como posibles inhibidores de la corrosión en aceros industriales [thesis]. Estado de México, Mexico: Universidad Autónoma del Estado de México; 2016
- [63] Franco M, Herrera-Hernández H, García-Orozco I, Herrasti P. Extracto acuoso natural de Morinda Citrifolia como inhibidor de corrosión del acero AISI-1045 en ambientes ácidos de HCl. *Revista de Metalurgia*. 2018;**54**(4):1-10. DOI: 10.3989/revmetalm.128
- [64] Rahayu EF, Asmorowati DS. Review of metal corrosion on food cans. *Journal of Physics: Conference Series*. 2019; **1321**:1-6. DOI: 10.1088/1742-6596/1321/2/022037
- [65] Geueke B, Groh K, Muncke J. Food packaging in the circular economy: Overview of chemical safety aspects for commonly used materials. *Journal of Cleaner Production*. 2018;**193**:491-505